Functionally distinct ERAP1 and ERAP2 are a hallmark of HLA-A29-(Birdshot) Uveitis.

Kuiper JJW[1,2,a], Setten J[3], Devall M[2], Cretu-Stancu M[4], Hiddingh S[1,2], Ophoff RA[5-7], Missotten TOAR[8], van Velthoven M[8], Den Hollander AI[9,10], Hoyng CB[9], James E[11], Reeves E[11], Cordero-Coma M[12], Fonollosa A[13], Adán A[14], Martín J[15], Koeleman BPC[4], de Boer JH[1], Pulit SL[4,16], Márquez A[17], Radstake TRDJ[2,18]

Short title: ERAP1 and ERAP2 in Birdshot Uveitis

Author Affiliations:

1. Department of Ophthalmology, University Medical Center Utrecht, University of Utrecht, Utrecht, the Netherlands.
2. Laboratory of Translational Immunology, University Medical Center Utrecht, University of Utrecht, Utrecht, the Netherlands.
3. Department of cardiology, University Medical Center Utrecht, University of Utrecht, Utrecht, the Netherlands.
4. Department of Genetics, Center for Molecular Medicine, University Medical Center Utrecht, Utrecht University, the Netherlands
5. Department of Psychiatry, Brain Center Rudolf Magnus, University Medical Center Utrecht, The Netherlands.
6. Department of Human Genetics, David Geffen School of Medicine, University of California, USA.
7. Center for Neurobehavioral Genetics, Semel Institute for Neuroscience and Human Behavior, University of California, USA.
8. The Rotterdam Eye Hospital, Rotterdam, The Netherlands.
9. Department of Ophthalmology, Donders Institute for Brain, Cognition and Behaviour, Radboud university medical centre, Nijmegen, the Netherlands.
10. Department of Human Genetics, Donders Institute for Brain, Cognition and Behaviour, Radboud University Medical Center, Nijmegen, The Netherlands.
11. Centre for Cancer Immunology, Faculty of Medicine, University Hospital Southampton, Southampton, UK.
12. Ophthalmology Department, Hospital de León, IBIOMED, Universidad de León, León, Spain.
13. Ophthalmology Department, BioCruces Health Research Institute, Hospital Universitario Cruces, Barakaldo, Spain.
14. Ophthalmology Department, Hospital Clinic, Barcelona, Spain.
15. Instituto de Parasitología y Biomedicina "López-Neyra", CSIC, PTS Granada, Granada, Spain.
16. Li Ka Shing Centre for Health Information and Discovery, Big Data Institute, Oxford University, Oxford, UK.
17. Systemic Autoimmune Disease Unit, Hospital Universitario San Cecilio, Instituto de Investigación Biosanitaria de Granada, Granada, Spain.
18. Department of Rheumatology and Clinical Immunology, University Medical Center Utrecht, Utrecht, The Netherlands.

a) To whom correspondence may be addressed. Email: J.J.W.Kuiper@umcutrecht.nl

Abstract

Recently, a family of inflammatory diseases have been proposed as comprising 'MHC-I-opathies, each hallmarked by a strong association with MHC-I. Birdshot Uveitis (*Birdshot*) is a rare eye condition that exclusively affects HLA-A29-positive individuals and could be considered a prototypic member of the MHC-I-opathy family. Genetic association studies have pinpointed the *ERAP1* and *ERAP2* genes as shared associations across MHC-I-opathies; the *ERAP* genes encode specialized enzymes that trim the N-terminus of peptides bound to MHC-I, a mechanism that suggests ERAP dysfunction may be a root cause for MHC-I-opathies. We mapped ERAP1 and ERAP2 allotypes across two European populations totaling 130 HLA-A29-positive Birdshot cases and 2,993 controls. We identified an association at variant rs10044354 (chr5q15) that mediated a marked increase in ERAP2 expression. We also identified and cloned a disease-associated ERAP1 allotype (tagged by rs2287987) present in 57% of cases; this allotype conferred significantly altered expression of ERAP1 isoforms in transcriptomic data (N = 360), resulting in lowered protein expression and distinct enzymatic activity. The combined rs2287987-rs10044354 haplotype associated with Birdshot more strongly than either SNP alone. Finally, we observed linkage disequilibrium between the ERAP1 and ERAP2 allotypes across European populations indicating that ERAP2 protein expression is dependent on the ERAP1 background. In conclusion, a functionally distinct combination of ERAP1 and ERAP2 are hallmarks of HLA-A29-associated Birdshot and provide rationale for strategies designed to correct ERAP function for treatment of Birdshot and MHC-I-opathies more broadly.

Words: 233

Author Summary

Birdshot Uveitis (Birdshot) is an eye disease that only affects HLA-A29-positive individuals. We found that polymorphisms in *ERAP* genes were strongly associated with Birdshot and substantially changed the expression and function of these enzymes. These observations designate Birdshot as a novel member of a recently proposed family of inflammatory conditions termed 'MHC-I-opathy' with shared molecular characteristics.

Introduction

'*MHC-I-opathy*' is a relatively new term proposed to unify a group of severe inflammatory diseases, each characterized by strong association with a unique major histocompatibility complex class I (MHC-I) allele and shared immune characteristics [1]. Recent genetic association studies revealed a vast enrichment for polymorphisms in the *endoplasmic reticulum aminopeptidase* (ERAP) genes, ERAP1 and ERAP2, in patients with *ankylosing spondylitis*, *psoriasis*, or *Behçet's disease* [2-5]. Importantly, in these conditions, *ERAP* is in epistasis with the risk alleles of MHC-I allele. However, not all patients with ankylosing spondylitis or Behçet's disease carry a MHC-I risk allele, an observation that has provoked discussions on this unifying concept [6,7] and whether it reflects shared underlying disease etiology.

The mechanism through which ERAP function contributes to MHC-I-opathies is still under intense discussion and the discovery of the underlying mechanism is hampered by several unique characteristics of these specialized enzymes: the peptidases ERAP1 and ERAP2 closely interact with MHC-I by contributing to the generation and destruction of peptides considered for presentation by MHC-I on the cell surface. This key function indicates that aberrant peptide processing by ERAP may be a root cause for MHC-I-opathies [8]. Similar to MHC-I, genetic diversity of *ERAP* genes is conserved by balancing selection [9]. Balancing selection maintains ERAP2 deficiency in one-quarter of the population [9] and drives the polymorphic *ERAP1* gene to encode various protein haplotypes (allotypes) [10], few of which paradoxically confer or reduce risk for developing MHC-I-opathies [8]. To date, ERAP allotype studies have been limited to the relatively more common MHC-I-opathies [11-13]. In contrast, Birdshot uveitis or *Birdshot chorioretinopathy* (from here on '*Birdshot'*) is a severe, extremely rare eye condition (~1-5 cases/500,000) [13,14] that is characterized by enhanced IL-23-IL-17 pathway activation [14-16], and occurs exclusively in HLA-A29-positive individuals [18]. A previous genome-wide association study in Birdshot highlighted strong involvement of the *ERAP* region on chromosome 5q15 [20]. The unique (diagnostic) prerequisite of HLA-A29 [19] and *ERAP* association classifies Birdshot patients within the MHC-I-opathy cluster and provides an attractive model to define the genetic architecture of this superfamily of conditions [18].

Therefore, we mapped ERAP1 allotypes and other key variants at 5q15 across two European populations of 130 cases and 2,993 controls, and interrogated their downstream implications using transcriptomic data, molecular cloning and functional assays.

Results:

Two independent variants at 5q15 associate with Birdshot

To test for genetic variants that associate with Birdshot, We obtained genotype data for 13 key variants at 5q15 in 84 cases and 890 controls from the Netherlands (**Supplementary Table 1)**. Using a logistic regression model, adjusted for sex and the top two principle components, we identified a top association at the T allele of rs10044354 in *LNPEP* (odds ratio (OR) = 2.42[95% CI: 1.69-3.45], $p = 1.21 \times 10^{-6}$, **Figure 1** and **Supplementary Table 1**). We accounted for the effect of rs10044354 using conditional analysis, and identified the C allele of rs2287987 (encoding valine at amino acid position 349) in *ERAP1* as a secondary (independent) association to Birdshot (OR = 1.99 [95% CI: 1.36-2.90], $p = 3.97 \times 10^{-4}$, **Figure 1**). Due to linkage disequilibrium (LD), several other SNPs across the locus also showed strong association, but conditioning on rs2287987 in *ERAP1* removed the remainder of the association signal in the region (**Supplementary Table 1**).

Naturally occurring ERAP1 protein haplotypes have been previously linked to MHC-I-opathies [8]. Considering 10 amino acid variants in *ERAP1* together [34], we identified 8

common (frequency >1%) haplotypes (**Table 1**). The Birdshot-associated C allele of rs2287987 (349V) resides in the ERAP1 haplotype previously labelled '*Hap10'* [34]. Indeed, testing for association of phased haplotype data revealed that *Hap10* was associated with Birdshot (OR= 2.23, $p = 2.5 \times 10^{-5}$, **Table 1**). We also noted that *Hap2* was less frequent in cases. Sixty-three percent of Birdshot cases had at least one copy of *Hap10* compared to 37% of controls (Fischer's exact test; OR = 2.88 [95%: CI 1.78-4.75], $p = 6.34 \times 10^{-6}$), while 13% of Birdshot cases were homozygous for *Hap10* compared to 3.7% of controls (OR=3.90 [95%CI: 1.71- 8.33], $p = 7.36 \times 10^{-4}$**, Supplementary Table 2**). Considered collectively, our association testing demonstrates that rs10044354 in *LNPEP* and rs2287987 (i.e. *Hap10*) of *ERAP1* explained the bulk of the association with Birdshot at 5q15.

Evidence for epistasis between HLA-A29 and a rs2287987-rs10044354 haplotype
We sought to replicate the associations with rs2287987/Hap10 and rs10044354 using a set of independent samples drawn from an independent Spanish cohort of 46 cases and 2,103 controls [35]. Both associations replicated (**Table 1** and **Supplementary Table 1**) and show consistent direction of effect. Interestingly, the risk haplotype rs2287987-C/rs10044354-T showed disease association exceeding the association for each individual SNP in both cohorts and is present in 50% of all 130 cases and 26% of all 2993 controls (**Supplementary Table 3**). The frequency of the CT-risk haplotype (0.24 in Dutch cases and 0.19 of Spanish cases) is ~5-6x less common in African (0.027%) and Asian (0.021%) populations compared to the European population (0.13%, **Figure 3A**). We investigated the possibility of interaction between the rs2287987-rs10044354 haplotype and HLA-A29 in combined 130 cases and 2993 controls. The CT-risk haplotype was associated with an odds ratio for Birdshot of 1.91 [95% CI 0.80-4.60] in HLA-A*29 negative versus an odds ratio of 17 [95% CI 9.51-30.4] in HLA-A*29 positive individuals (**Figure 3B**).

Non-random distribution of ERAP1-ERAP2 haplotypes in the European population.
ERAP2 encodes two common haplotypes [9]: the A allele of rs2248374 tags Haplotype A [*HapA*], which encodes a canonical protein, while the G allele tags *HapB,* which lacks functional protein (**Supplementary Figure 6**). Since ERAP1 is postulated to be complemented by ERAP2 in trimming peptides [36], we hypothesized that the expression of ERAP2 protein could be dependent on the *ERAP1* haplotype and that this relationship should be evident in the population. To explore this hypothesis, we used phased genotype data of 2,993 controls to test whether the frequency of *HapA* of *ERAP2* differed between *ERAP1* haplotypes encoded along the same chromosome. We observed a non-random distribution of *ERAP2-HapA* across the *ERAP1* haplotypes in several European populations (**Figure 2** and **Supplementary Table 4**). This reflects the complex pattern of mild to high LD (D') between amino acid variants in *ERAP1* and rs2248374 in *ERAP2* (**Supplementary Figure 7**). A similar non-random distribution was observed for *ERAP1* haplotypes based only on five amino acids [12] (**Supplementary Figure 8**). This demonstrates that the co-occurrence of functional ERAP2 protein is dependent on the ERAP1 allotype background.

The primary association signal at 5q15 associates with increased ERAP2 expression
Next, we aimed to predict the local transcriptional regulation of the Birdshot-associated loci at 5q15 using RNA-sequencing data from 360 individuals of European ancestry and 82 individuals from African ancestry. We used lymphoid cell lines due to their high expression of ERAPs and representation of expression quantitative trait loci (eQTLs) cis effects of blood cell populations (**Supplementary Figure 9**). We applied a linear mixed model controlling for sex, ancestry, and batch to model if the SNPs imposed eQTLs effects on transcripts encoded by 5q15 (**Figure 3C**); The leading SNP (rs10044354) in *LNPEP* was not associated with the expression of its major transcript (**Supplementary Table 5**). We extracted common missense and splice region variants of *LNPEP* in high LD with rs10044354 from the European populations of the 1000 Genomes [29] and identified the splice region variant

rs3836862 (r^2>0.96 in 5 populations) located near the exons encoding the zinc-binding motif of the enzyme and is predicted to influence splicing. However, we detected no evidence for potential alternative splicing of *LNPEP* by this variant in lymphoid cell lines (**Supplementary Figure 5**). Correcting for the expression of ERAP2 mediated by rs2248374, we found the risk allele of rs10044354 to be strongly associated with *ERAP2* in sample from European Ancestry. Further, this allele associated to a 235% increase in expression of *ERAP2* independent from rs2248374 (IRR^2 [95% CI]= 3.35[2.76-4.06], p = 3.48 x 10^{-33}, **Table S5, Figure 3D**). In line with this, conditioning on rs2248374 in *ERAP2* in the 130 cases and 2993 controls combined, we found the association for rs10044354 with Birdshot to be independent from rs2248374 (p = 9.1 x 10^{-4}).

ERAP1 risk alleles reside in a relatively low expressed allotype

The Birdshot risk variant rs2287987 (349V in ERAP1) is in near complete LD (r^2=0.99) with rs10050860 (575N in ERAP1, p = 1.46 x 10^{-6} for association with Birdshot). The SNP rs10050860 was recently suggested to represent a splice interfering variant (rs7063), which was linked to changes in the proportion of expression of two major ERAP1 isoforms [31]. We explored the rs7063 variant using rs1057569 (r^2=1). Indeed, we observed strong association between the rs1057569 genotype and the expression of the two major *ERAP1* transcripts in samples of European ancestry (**Supplementary Table 5**). This variant is also among the top eQTLs for *ERAP1* in lymphoid cell lines investigated in the GTEx project (**Supplementary Figure 10**). The rs2287987 is in moderate LD with rs1057569 (r^2 = 0.55) and associated with ~50% change in expression of the major ERAP1 isoform (**Supplementary Table 5** and **Figure 3E**), which results in ~5x lower cumulative levels of ERAP1 protein in HLA-A29-positive individuals homozygous for the C allele of rs2287987 (**Figure 3F**). However, the eQTL effects of rs2287987 on *ERAP1* transcripts were completely abrogated once adjusted for rs1057569 (**Supplementary Table 5**). Therefore, we tested whether the rs2287987 disease signal was mediated by rs1057569. Conditioning on rs1057569, we found the rs2287987 signal to be modestly affected (p_{meta} = 4.61 x 10^{-4}), while conditioning on rs2287987 neutralized the signal (p_{meta} = 0.39). These results indicate that the association signal at rs2287987 represents a signal beyond the association with the splice interfering variants in *ERAP1*. We note that the A allele of rs1057569 (T allele of rs7063) associated with low expression of ERAP1 protein co-occurred >90% of Hap10 and Hap6, and <10% of the other ERAP1 protein allotypes in controls. In the Nigergian (YRI) population (n=82), the rs2287987 genotype is not in LD with rs1057569 (r^2= 0.009), and not linked to ERAP1 expression (transcript ENST00000443439.6, IRR^2 [95% CI]= 0.93[0.65-1.32], p = 0.68).

Full-length ERAP1 sequencing of the risk allotype

We cloned the full-length coding sequence of *ERAP1* from two patients that were heterozygous or homozygous for *Hap10* to reveal the amino acid residues for additional reported amino acid positions in ERAP1 [37]. Analysis of the coding sequence revealed that both copies (based upon 9 individual clones) of *Hap10* encoded the ancestral alleles for additional reported amino acid positions (**Supplementary Table 6**). All detectable transcripts contained a C-terminus identical to the 19-exon transcript ERAP1-202 (ENST00000443439.6).

Disease-associated ERAP1 displays distinct enzymatic activity.

Considering the association of rs2287987 exceeded variants that govern *ERAP1* expression and that rs2287987 has previously been shown to affect trimming properties of recombinant ERAP1 [38,39], we assessed the relative enzymatic activities of ERAP1 allotypes *in vitro*. We compared normalized concentrations of ERAP1 protein precipitated from lymphoid cell lines of patients and controls that carry the *Hap10* and *Hap2,* the latter haplotype showing evidence for protection against Birdshot (**Table 1**). Total cellular ERAP1 protein appeared to

have slower rates for enzymatic trimming of the archetypical fluorogenic substrate *L-Leucine-4-methylcoumaryl-7-amide* (Leu-AMC) with each sequential increase in Hap10 compared to homozygous carriers of *Hap2* (**Figure 3G**). These results confirm that changes of enzymatic properties in ERAP1 are mediated by haplotypes that carry the C allele of rs2287987 (i.e., *Hap10*), thereby governing functional consequences for patients with Birdshot.

Discussion

We defined the common *ERAP1* and *ERAP2* haplotype structure in Birdshot, we confirmed the genetic association with rs10044354 [20] and showed that despite strong LD between rs10044354 and splice region variant rs2248374 in *ERAP2*, the strong eQTL effects of rs10044354 on ERAP2 expression are independent from rs2248374. This finding suggests that a change in expression, and not merely the presence of ERAP2, confers risk for Birdshot and other ERAP2-linked conditions [40]. Thus, future treatment strategies to dampen ERAP2 expression may complement current research efforts focused on the pharmacological inhibition of its aminopeptidase activity [41,42].

We revealed a second independent association for rs2287987 in *ERAP1*, a SNP that nearly always resides in the common ERAP1 haplotype *Hap10* [34]. The rs2287987 risk genotype is accompanied by changes in *ERAP1* transcript levels and lower protein expression as a result of LD with rs1057569, a strong eQTL for *ERAP1* (**Supplementary Figure 10**). The functional implications of ERAP1 expression need further investigation, especially since the risk genotype linked to *ankylosing spondylitis* (AS) results in increased ERAP1 expression [31]. However, the association with rs2287987 was independent from rs1057569, suggesting disease modifying effects beyond the expression of ERAP1. Indeed, we ascertained that the Birdshot-associated allele of rs2287987 (349V located near the zinc-binding motif of the enzyme) resides in an allotype that within cells exhibits distinct enzymatic activity and our data support previous studies indicating that Hap10 can be considered functionally antagonistic to Hap2 and Hap1 [37,39]. Also, direct comparison by molecular cloning revealed that *Hap10* in Birdshot and a previously investigated 15-amino acid ERAP1 haplotype, termed **001,* represent identical ERAP1 allotypes [10,37]. The *001 (Hap10) was previously shown to provide suboptimal peptide cargo for MHC-I, by reduced trimming of peptides [10,37]. Therefore, Hap10 may confer risk by incomplete destruction

of immunogenic or insufficient generation of protective epitopes that bind HLA-A29. Eye tissues of Birdshot patients are infiltrated by $CD8^+$ T cells, but to date, evidence for their direct involvement is lacking [18]. ERAP1 and ERAP2 may perhaps also influence T or NK cells function via *Killer immunoglobulin-like* (KIR) receptors, a class of immune receptors that interact with MHC-I that have been genetically linked to Birdshot [43].

Hap10 plays a central role for patients within the MHC-I-opathy cluster: Hap10 is the major risk ERAP1 allotype for patients with *Behçet's Disease* (BD) and is highly protective against AS (i.e. Hap1/Hap2 are risk haplotypes for AS)[11,12]. Hap10 is associates with BD assuming a recessive model (Birdshot, $p_{meta\text{-}recessive} = 9.81 \times 10^{-5}$). Interestingly, AS and BD commonly manifest with uveitis [11,44] and the *ERAP1* associations are much stronger in cases that developed uveitis compared with cases with systemic disease alone [2,44]. Although HLA-A29 is also common in some non-European populations, Hap10 and particularly the Hap10-ERAP2 (rs2287987-rs10044354) haplotype are less common in Asian and African individuals compared to European and may exhibit different functional effects on ERAP1, which may partly explain why Birdshot primarily affects patients of European descent [18].

Although 90% of all cases carried either a risk allele for rs2287987 or rs10044354, 50% of all cases were positive for the combined haplotype. A proportion of Birdshot patients may have self-limiting disease, while others will develop irreversible retinal dysfunction and blindness [13]. It will be interesting to evaluate the potential relation between *ERAP* haplotypes and clinical outcome (e.g., electroretinography) in follow-up studies. This was not possible because of the relatively limited sample size, owing to low prevalence of this rare disease [13,14]. This limitation also hampered the investigation for association with other SNPs with evidence for more moderate effect size (e.g. rs30187). Regardless, we observed the strongest association for the rs2287987-rs10044354 haplotype and HLA-A29, a triad of genes that encode functionally tightly related proteins of the antigen presentation pathway and warrants further investigation of this antigen processing pathway in uveitis. Whether ERAP1 and ERAP2 contribute to disease by direct interaction in the endoplasmic reticulum is not known [36,42,46]. In the absence of ERAP2 protein, cells with distinct *ERAP1* haplotypes show substantial differences in HLA-A29 peptidome composition, which demonstrates that ERAP1 is able to directly influence HLA-A29 [45]. Also, ERAP2 has different peptide preferences compared to ERAP1 [36,41] and MHC-I peptidome studies support separate contributions of Hap10 and ERAP2 in manipulating the peptide composition presented on the cell surface [46]. This reflects the lack of LD between the protein-coding *ERAP2* haplotype and MHC-I-opathy linked Hap10 and Hap2/Hap1 in ~3000 controls. However, ERAP2 protein expression more often occurs in *ERAP1* haplotypes Hap8 and Hap7 (and perhaps Hap3) background, as a result of LD (D') between SNPs including rs3734016, and rs26618 and rs2248374 (**Supplementary Figure 7**). The lack of detailed MHC-I data hampered further investigation of this phenomena, because ERAP2 may not equally contribute to the peptidome of each MHC-I molecule [39,46]. However, this would demand a large population study with sufficient power to investigate the ERAP1-ERAP2 haplotypes for distinct MHC-I haplotypes. Such studies will also be key to advance our understanding of ERAP function in inflammation, cancer, and less explored fields such as transplantation biology and vaccine efficacy studies.

The original concept of the MHC-I-opathy aims at clustering subsets of clinical phenotypes on the basis of one or multiple unifying molecular fingerprints [1]. Here, we explicitly refer to the subgroup of patients that carry risk MHC-I alleles (and ERAP variants in epistasis) when referring to 'MHC-I-opathy' patients. Our results in Birdshot further substantiate the existence of such concept. We envision that molecular reclassification based on a patient's MHC-I and ERAP haplotype may improve clinical decision making as well as drug discovery

(e.g. ERAP inhibitors) in the near future. Emerging studies explore this concept, those of which that have linked clinical response to *ERAP* variants [48-51]. Ultimately, understanding how to pharmacologically influence ERAP function [52] may lay the foundation for the design of effective therapeutic strategies to correct ERAP function in accordance with the patient's molecular fingerprint to tailor the treatment of MHC-I-opathy patients specifically.

Methods

5q15 variant and haplotype testing in Dutch and Spanish cohorts

This study was performed in compliance with the guidelines of the Declaration of Helsinki and has the approval of the local Institutional Review Board (University Medical Center Utrecht). Genotype data for 13 key variants at 5q15 (**Supplementary Table 1**) and HLA-A29 status from 84 Dutch cases and 890 Dutch controls from European ancestry were obtained from a previously-described discovery collection and the Genome of the Netherlands Project (GoNL) release 4 [20,21]. The number of samples is slightly fewer than the Dutch discovery cohort because some samples no longer met the criteria for Birdshot Uveitis (e.g., presence of systemic disease) or failed to pass quality control requirements. Imputation of untyped SNPs was conducted using the GoNL and 1000 Genomes Project Phase 3 data (imputed SNPs with info>0.95) [22]. Disease association testing was performed with PLINK v1.07 [23] using a logistic regression model correcting for the top two principal components and sex (**Supplementary Figure 1**). For replication, the genotype data (n=13) (**Supplementary Table 1**) and HLA-A29 status were extracted from 46 Spanish cases and 2,103 Spanish controls from a previously-described non-infectious uveitis collection [24] and tested with a logistic regression model (replication was defined as Bonferroni-corrected p-value for 2 LD blocks at 5q15 = 0.025). Meta-analysis of Dutch and Spanish cohorts was performed using inverse variance-weighted meta-analysis [25]. Common ERAP1 allotypes (10-amino acid haplotypes, which occur in >1% of controls) were phased using PLINK. The estimated haplotype frequencies for the identified 8 common ERAP1 allotypes (**Supplementary Figure 2)** matched the frequency of haplotypes estimates of genotype data by *SHAPEIT2* (considered the most accurate method available [26]). Therefore, the phasing accuracy of PLINK was considered sufficient for *ERAP1* haplotype association testing using logistics regression (**Supplementary Figure 3**). The total testing burden for SNP association was estimated at ([13 variants + 8 ERAP1 protein allotypes] x 3 models + 4 rs2287987-rs10044354 haplotypes = 67 independent tests) a 1% type I error rate with $p<1.49 \times 10^{-4}$, which was used as a threshold to prioritize SNP associations calculated in the discovery and meta-analysis. We tested for interaction between HLA-A29 and the rs2287987-rs10044354 haplotype using a logistic regression model by computing a parameter for HLA-A29 status (positive or negative). The odds ratio for each haplotype in the presence or absence of HLA-A29 is calculated compared to the protective rs228987-T-rs10044354-C haplotype in the absence of HLA-A29.

Investigation of the distribution of ERAP1 and ERAP2 haplotypes in European populations

The major haplotype of *ERAP2* is under balancing selection, where the G allele rs2248374 tags a non-protein coding haplotype [HapB] and the A allele of rs2248374 tags the protein-coding haplotype [HapA] [9]. The frequency of the A allele of rs2248374 co-occurring on the same chromosome with each of the eight common ERAP1 haplotypes was determined in the 890 Dutch and 2103 Spanish controls using phased haplotype data using SHAPEIT2 [26], and phased haplotype data were obtained for the British [GBR], Finnish [FIN], Utah residents with Northern and Western European Ancestry [CEU], and Tuscany [TSI] populations from the GEUVIDAS consortium [27]. The 95% confidence intervals of the observed frequencies were estimated using bootstrap sampling (n=20,000). We used a two-sided exact binominal test to assess whether the observed frequencies were non-random (deviation from a test probability of 0.5 or the hypothesis that ERAP2 co-occurs in 50% of

any particular ERAP1 haplotype). Frequency distribution of ERAP2 for each of the ERAP1 haplotypes was considered non-random at [A or G rs2248374 for 8 ERAP1 haplotypes = 0.05/16] $p<2.5 \times 10^{-3}$ in both the Dutch and Spanish populations (with consistent direction of effect).

Statistical framework for 5q15 eQTL analysis

To investigate the transcriptional regulation of the variants at 5q15, RNA-sequencing data from the GEUVADIS consortium of 360 lymphoid cell lines of European ancestry and 82 African samples [27] were extracted via the *recount2* package, a resource for expression data for uniformly processed and quantified RNA-sequencing reads from >70,000 human samples [28]. Transcript-level counts of all samples of the GEUVADIS study were scaled using the `scale counts` function in the recount2 package to take into account differing coverage between samples. Data corresponding to reported transcripts from *ERAP1*, *ERAP2*, and *LNPEP* (n=25 using *Ensembl* transcript IDs) were extracted for all samples, of which 4 transcripts were sufficiently expressed and considered for testing the effect of genotype on transcript expression (ERAP1~201, ENST00000296754.7; ERAP1~202, ENST00000443439.6; ERAP2~202, ENST00000437043.7; LNPEP~201, ENST00000231368.9). The phased genotype data were obtained via the *Ensembl* portal [29]. To interrogate the effect of genotype on local transcript expression, we fitted a generalized linear mixed model (GLMM) using a negative binominal fit of the count data and logarithmic link using the *lme4* package in R (v3.3.2)[30], with a fixed effect of patients sex and random effects of laboratory (n=7) and population (n=5) of the 1000 Genomes project (formula 1). For pairwise conditioning, the genotype of the studied SNP was added as a covariate into the GLMM (formula 2):

```
(1):  glmer.nb(expression ~ genotype + sex  +(1|Laboratory)+(1|Population))

(2):  glmer.nb(expression ~ genotype + sex  + conditional SNP genotype +
      (1|Laboratory)+(1|Population))
```

Genotypes were ranked using their imputed dosage value (a number from 0 to 2, indicating the number of risk alleles for each SNP; **Supplementary Table 1**) adapted from a previous method [31]. Patients homozygous for the G allele of rs2248374 (n=94) were removed to fit a model for ERAP2 expression in HapA-positive individuals. The incident rate ratio (IRR) is the exponential of the coefficient returned from the GLMM. We used IRR^2 as the metric for change in transcript expression, which is conceptually similar and close to fold the change in expression (mean count of the transcript) between individuals homozygous for the protective over individuals homozygous for the risk alleles. IRR^2 <0.60 or >1.30 (>30% change in expression) were prioritized for reporting as biologically relevant. Effect size metrics of eQTL analysis from lymphoid cell lines and whole blood from the *Genotype-Tissue Expression* (GTEx) project Phase 2 for genes at 5q15 were obtained via the GTEx portal [32].

Western blot analysis of ERAP1 and ERAP2

Human lymphoid cell lines were generated from peripheral blood of Dutch cases recruited at the Departments of Ophthalmology at the University Medical Center Utrecht and Radboud University Medical Center, the Netherlands. Cells were grown in Roswell Park Memorial Institute (RPMI) 1640 medium supplemented with 10% heat-inactivated fetal bovine serum and antibiotics. The following HLA-A29-positive cell lines were obtained from the *National Institute of General Medical Sciences* (NIGMS) Human Genetic Cell Repository at the Coriell Institute for Medical Research: GM19310, GM19397, GM19452, HG00096, HG00113, HG00116, HG01082. Protein lysates (10µg/lane) of $>2 \times 10^6$ cells were separated on a 4-20% Mini-PROTEAN TGX gel (Bio-Rad Laboratories) and transferred to a Polyvinylidene

difluoride (PVDF) membrane and detected using antibodies to ERAP1 and ERAP2 (AF3830, AF2334, both R&D Systems), and α-tubulin (T6199, Sigma), and secondary antibodies conjugated to Horseradish Peroxidase. The ratio of the intensity of the ERAP1 over α-tubulin band was calculated using Image Lab 5.1 (Bio-Rad Laboratories) and grouped according to the distribution of rs2287987 genotype. Details on the Western blot analyses of lymphoid cell lines are outlined under **Supplementary Figure 4**.

LNPEP sequencing
We sequenced exon 5-8 of *LNPEP* from total RNA (cDNA) in steady-state or 24 hour stimulated (TLR7/8 [R848] and TLR9 [CpG-B ODN 2006] agonists) lymphoid cell lines of 4 individuals homozygous for the deletion and 4 homozygous for the C allele of rs3836862, as determined by sanger sequencing. Detailed methods and used primers are provided in **Supplementary Figure 5**.

Full-length ERAP1 cloning and sequencing
RNA was isolated from >2 × 10^6 cells of two patients with Quick-RNA™ MiniPrep kits (Zymo Research) and immediately used to generate cDNA with the Transcriptor High Fidelity cDNA synthesis kit (Roche) using the provided random hexamere primers. *ERAP1* was directly amplified from cDNA as described [10]. The product was gel-purified, and cloned into the blunt-end cloning vector, pCR-Blunt II, using the Zero Blunt ® TOPO ® PCR Cloning kit (Life Technologies) or cloned into StarGate® pESG-IBA vectors (IBA Lifesciences), and sequenced.

Cellular ERAP1 enzymatic activity
Total cellular ERAP1 was immuno-precipitated with anti-ERAP1 (5ug/mL, AF2334, R&D Systems) antibody and protein G-sepharose beads as described [32]. Equivalent concentrations of protein samples (normalized by Bradford assay) of purified ERAP1 were incubated with 50µM Leucine-aminomethylcoumarin (L-AMC) and fluorescent intensity was followed for 30 minutes with excitation at 365/380nM and emission at 440/450nm.

Acknowledgement
We would like to thank prof. Aniki Rothova for support in evaluation of Birdshot patients.

Funding Statement

JJWK and SLP are supported by a VENI Award from the Netherlands Organization for Scientific Research (N.W.O. project numbers 016.186.006, and 016.186.071). AM is recipient of a Miguel Servet fellowship (CP17/00008) from the Spanish Ministry of Economy, Industry and Competitiveness. JJWK was supported by unrestricted grants of the Fischer Stichting, the Landelijke Stichting voor Blinden en Slechtzienden, and the Algemene Nederlandse Vereniging ter Voorkoming van Blindheid, that contributed through *UitZicht*. The funding organizations had no role in the design or conduct of this research.

Figure Legends

Figure 1 | Association and conditional testing for the 13 polymorphisms at 5q15. A. Initial association testing mapped the strongest association to rs10044354 in *LNPEP* (Dark red). **B.** Conditioning on rs10044354 revealed independent association for the C allele of rs2287987 (amino acid position 349 in ERAP1) and variants in tight LD (rs10050860 and rs17482075 in dark blue) in *ERAP1*. **C.** Conditioning on both rs10044354 and rs2287987 removed the bulk of the signal (rs30187, p = 0.05). Plot framework was generated by *LocusZoom* and edited for graphical purposes.

Figure 2 | Non-random distribution of the ERAP2-protein coding haplotype across common ERAP1 allotypes. Ten missense variants in *ERAP1* encode eight discrete and common haplotypes, while *ERAP2* encodes 1 common protein-coding haplotype (*HapA* tagged by the A allele of rs2248374) and a non-coding haplotypes (tagged by the G allele). Each chromosome 5 harbors one ERAP1 haplotype and one ERAP2 haplotype. Using phased ERAP1-ERAP2 haplotype data of 890 Dutch controls (1780 phased haplotypes) and 2103 Spanish controls (4206 phased haplotypes), we outlined the percentage of *HapA* per ERAP1 haplotype on the same chromosome. Error bars indicate the 95% confidence interval based upon 20,000 bootstrap samples. Frequency of *HapA* of ERAP2 for each of the ERAP1 haplotypes was considered non-random if the observed frequency deviated from an expected 50% using an exact binominal test with [A or G rs2248374 for 8 ERAP1 haplotypes = 0.05/16] $p<2.5 \times 10^{-3}$ in both the Dutch and Spanish populations with consistent direction of effect. ERAP1 haplotypes that fulfilled these criteria are highlighted by asterisks (for summary statistics see Supplementary Table 4). As a reference, we plotted the ERAP1-ERAP2 haplotype data for the 360 samples from the CEU, FIN, GBR, and TSI populations from the 1000 Genomes sample collection used for functional investigation in this study [27].

Figure 3 | Birdshot associated variants affects ERAP1 and ERAP2 expression and function. A. The frequency of the rs2287987-rs10044354 haplotypes in Dutch and Spanish cases and controls, and the EUR, EAS, and AFR super populations of the 1000 Genomes project [27]. The frequency of the haplotypes is indicated as the percentage of all haplotypes for each population. **B**. We tested for ERAP haplotype association and HLA-A29 status in the combined Dutch and Spanish samples. Odds ratios for Birdshot were calculated relative to lowest risk genotype (the protective haplotype rs2287987-T/rs10044354-C with a negative HLA-A29 status was set to an odds ratio of 1). The risk allele (red) and protective allele (green) are highlighted. **C.** Expression data for transcripts at 5q15 in 360 lymphoid cell lines from the European populations from the GEUVIDAS consortium [27]. Red lines indicate the median expression **D.** The lead SNP rs10044354 is a strong eQTL for ERAP2 independent of rs2248374 (details eQTL analysis in Supplementary Table 5). **E.** The Birdshot-associated rs2287987 is associated with changes in the two major ERAP1 transcripts. **F.** Quantitative Western blot analysis of the protein expression of ERAP1 in HLA-A29-positive cell lines according to the distribution of rs2287987 (more details see *Supplementary Figure 7*). **G.** Hydrolysis (expressed as relative fluorescent units [RFU] of the substrate *Leu-AMC* by immuno-precipitated ERAP1 protein from lymphoid cell lines homozygous *Hap10* (risk allotype), homozygous *Hap2* (protective allotype) and a heterozygous donor for these two *ERAP1* haplotypes. Error bars indicate the mean (range) of three independent experiments.

Supporting Information Legends

Supplementary Figure 1 | Analysis of genetic matching of cases and controls. Principle component analysis (PCA)first versus second and second versus third component in cases and controls using genotype data from the Dutch collections as described in method section. PCA was computed using a set of random 75,239 independent SNPs autosome-wide (chr 1-22) in EIGENSOFT (*Price et al. Principal components analysis corrects for stratification in genome-wide association studies. Nat Genet. 2006 Aug;38(8):904-9*), excluding the *MHC*, two large inversions on chromosomes 8 and 17 and the *LCT* locus on chromosome 2. The SNPs all had a minor allele frequency (MAF) <0.1, were not in Hardy-Weinberg equilibrium ($p < 10^{-4}$) and showed a pairwise LD of 0.2 or less.

Supplementary Figure 2 | Three-dimensional surface model for the ERAP1 allotype associated with Birdshot uveitis (Protein Data Bank entry: 3MDJ). Common variant amino acid residues in ERAP1 are displayed as spheres; Ancestral amino acids are highlighted in green and non-ancestral amino acid positions are highlighted in red. 3D structure was produced using UCSF Chimera (*Pettersen, E. F. et al. UCSF Chimera - a visualization system for exploratory research and analysis. J. Comput. Chem. 25, 1605–1612 2004*).

Supplementary Figure 3 The estimated haplotype frequency (%) for the 8 common ERAP1 haplotypes using Plink and SHAPEIT for cases (in red) and controls (in green). The dotted diagonal line indicates perfect correlation between the estimated haplotype frequencies.

Supplementary Figure 4 | ERAP1 and ERAP2 expression in B cell lines of Birdshot uveitis and HLA-A29-positive controls. We assessed ERAP1 and ERAP2 protein levels in EBV transformed B cells (EBV-LCL), from twelve HLA-A*2902-positive individuals (except NA11994) from the 1000 Genomes project and EBV-LCLs generated from peripheral blood mononuclear cells of four BU patients genotyped in this study, by western blotting. Protein lysates (10µg/lane) from cells were separated on a 4-20% Mini-PROTEAN TGX gel (Bio-Rad Laboratories) and transferred to a PVDF membrane. Proteins were detected using a 1:5000 dilution of primary antibodies; goat anti-ERAP2 polyclonal antibody (AF3830, R&D Systems), goat anti-ERAP1 polyclonal antibody (AF2334, R&D Systems) and anti-α-tubulin monoclonal prepared in mouse (T6199, Sigma). Anti-mouse secondary antibody conjugated to Horseradish Peroxidase (HRP) (Jackson ImmunoResearch; 1:5000) and anti-goat secondary antibody conjugated to HRP (DAKO; 1:5000) were used to probe primary antibodies. Protein bands were detected with Amersham Prima Western Blotting (RPN22361, GE Healthcare) on the ChemiDoc Gel Imaging System (Bio-Rad Laboratories). Independent experiments are individually outlined below for ERAP1. The ratio of the intensity of the ERAP1 over α-tubulin band was calculated using Image Lab 5.1 (Bio-Rad Laboratories) for each experiment. All ratios of the intensities were grouped according to the distribution of *Hap10* (red = homozygous for rs2287987-C, orange = heterozygous for rs2287987-C, green is non-carriers) for quantitative analysis as outlined in **Figure 3F**.

Supplementary Figure 5 | rs10044354 is in tight LD with a splice region variant in LNPEP. We searched the 5 European populations (British [GBR], Iberian [IBS], Finnish [FIN], Utah residents with Northern and Western European Ancestry [CEU], and Tuscany [TSI]) of the *1000 Genomes Project* for missense or splice region variants of *LNPEP* in high LD (r^2 >0.75) with rs10044354; The rs10044354 variant is in tight LD (r^2 >0.96-1.0) with rs3836862 located in the splice region of intron 6-7 of *LNPEP*. These exons encode the key Zn-binding motif of the enzyme. The *Human splicing finder* software (http://www.umd.be/HSF3/) predicted a potential impact of the rs3836862 on splicing of this region. To explore if rs3836862 altered splicing of intron-6-7, we tested if the presence of rs10044354/rs3836862 affects the sequence of the predominant mature transcripts near this splice region. We selected four lymphoid cell lines that were homozygous null and four homozygous carries of the C allele of rs3836862 (as determined by Sanger sequencing). For each cell line, a total of 1×10^6 cells were cultured in 2 mL RPMI 1640 (Life Technologies), supplemented with 10% (v/v) heat-inactivated FCS (Biowest) and 1% (v/v) penicillin and streptomycin (Life Technologies) in a six wells plate for 24 hours and stimulated with TLR agonists resiquimod (*R848*; 1 µg/ml), or CpG-B (*ODN684*; 5 µM, both from *InvivoGen*), or left untreated. Total RNA was extracted using QiaCube and RNeasy mini kit (*Qiagen*) and a 443 bp cDNA fragment from exon 5 to exon 8 of *LNPEP* was generated by SuperScript ® cDNA synthesis kit (Invitrogen, UK) using 5'-3' (forward) TATGCCTTGGAAACAACTGTGA and 5'-3'(reverse) TGTTCTGAAGACTGAACAGA TGAT. A 438 bp cDNA fragment was amplified

using proof reading Pfu DNA polymerase-PCR reaction (Agilent Technologies, Santa Clara, CA, USA) with 5'-3'(forward) TGCCTTGGAAA CAACTGTGAAG and 5'-3' (reverse) TCTGAAGACTGAACAGATGATGA. A single band was detected in all conditions by agarose gel and sequenced at Macrogen Europe (Netherland) with 5'-3'(forward) GGAAACAACTGTGAAGCTTCTTGA and 5'-3'(reverse) CTTTCTTCATGGTTTT AAATCGAGC. Chromatograms from representative donors (unstimulated) from each group are indicated below. These analyses detected a sequence identical to the canonical transcript of *LNPEP* (Ensemble ID *ENST00000231368*) in all samples. We concluded that rs3836862 does not affect the sequence of the predominant (detectable) mature LNPEP transcripts in lymphoid cell lines under the described conditions.

Supplementary Figure 6 | The common splice region variant of *ERAP2* tags the bimodal distribution of protein expression. *ERAP2* encodes at least two common haplotypes that are tagged by rs2248374. The A allele tags the protein-coding haplotype (HapA), while the G allele tags a haplotype that encodes a transcript that is usually prone to none-sense mediated decay [9] and loss strongly reduced protein expression. Expression of ERAP2 in CEPH controls according to rs2248374 genotype is provided for three B-cell lines from individuals from the CEPH panel (*Dausset J. et al. Centre d'etude du polymorphisme humain (CEPH): collaborative genetic mapping of the human genome. Genomics. 1990;6:575–577*). Genotype information was obtained from the *Ensembl Genome Browser* (rs2248374 or rs2549797 that is in full LD [r^2 =1] with rs2248374). Cells were lysed and ERAP2 expression was assessed after SDS–PAGE and western blotting with antibodies to ERAP2. The endogenous levels of β-tubulin protein were analyzed as a loading control.

Supplementary Figure 7 | Linkage disequilibrium across the 13 polymorphisms in *ERAP1* and *ERAP2* in cases and controls. **Left**: The linkage disequilibrium across the functional variants at 5q15. The heatmaps show the D'prime and r^2 values calculated for SNPs in the Dutch and Spanish controls.

Supplementary Figure 8 | Non-random distribution of the ERAP2-protein coding haplotype across common ERAP1 haplotypes based on 5 SNPs. Five missense variants in *ERAP1* encode four discrete and common (>1% freq) haplotypes [12], while *ERAP2* encodes 1 common protein-coding haplotype (*HapA* tagged by the A allele of rs2248374) and non-coding haplotypes (tagged by the G allele). Each chromosome harbors 1 ERAP1 haplotype and 1 ERAP2 haplotype. We outlined the percentage of *HapA* per ERAP1 haplotype on the same chromosome using phased ERAP1-ERAP2 haplotype data of 890 Dutch controls (blue) and ERAP1-ERAP2 haplotype data for the 360 samples from the CEU, FIN, GBR, and TSI populations (grey) from the 1000 Genomes sample collection used for functional investigation in this study [27].

Supplementary Figure 9 | The normalized effect size from the eQTL analysis for variants at 5q15 derived from the Genotype-Tissue Expression (GTEx) Project. Data for 117 lymphoid cell lines and 369 whole blood samples were obtained from the GTExportal (GTEx Analysis Release V7) as described in the method section.

Supplementary Figure 10 | eQTL data for variants in ERAP1 and ERAP2 in lymphoid cell lines of 117 individuals from the Genotype-Tissue Expression (GTEx) Project. P values from eQTL analysis for ERAP1 and ERAP2 were obtained from the Genotype-Tissue Expression (GTEx) [32] Project (GTEx Analysis Release V7). The eQTLs for ERAP1 and ERAP2 identified in this study are indicated. Hg19 EUR 2014 1000 genomes LD structure. Plots were generated in LocusZoom [52].

Supplementary Table 1 | Association results for common functional variants at 5q15 in ERAP1, ERAP2 and LNPEP genes in Dutch and Spanish populations.

Supplementary Table 2 | Distribution of Hap10 in the Dutch and Spanish cases and controls. The frequency of the rs2287987-C (i.e. Hap10+ individuals) or rs2287987-CC (i.e. Hap10 homozygous individuals) genotypes in cases and controls was tested by Fischer's exact test. OR; odds ratio. 95%CI; 95% confidence interval.

Supplementary Table 3 | Results of test for association of the haplotype rs2287987 (risk allele C) and rs10044354 (risk allele T) with Birdshot Uveitis in 130 cases and 2993 controls using a logistic regression model.

Supplementary Table 4 | The frequency of the rs2248374 A allele in *ERAP2* co-occurring with each of the 8 common ERAP1 haplotypes is non-random in phased haplotype data of 890 Dutch and 2103 Spanish controls. The *ERAP2* protein-coding haplotype [11] is tagged by the A allele of rs2248374 in *ERAP2*. We used a two-sided exact binominal test to assess if the observed frequencies were non-random (deviation from a test probability of 0.5 or the hypothesis that ERAP2 co-occurs in 50% of any particular ERAP1 haplotype). Frequency distribution of ERAP2 for each of the ERAP1 haplotypes was considered non-random if the frequency deviated at a significant level of [A or G rs2248374 for 8 ERAP1 haplotypes = 0.05/16] $p<2.5 \times 10^{-3}$ in both the Dutch and Spanish populations (with consistent direction of deviation from 50%). ERAP1 haplotypes that fulfilled these criteria are highlighted (in orange haplotypes that more frequently co-occur with rs2248374-A allele and in blue haplotypes that less frequently co-occur with rs2248374-A allele).

***Supplementary Table 5* | Birdshot-associated SNPs are eQTLs for *ERAP1* and *ERAP2* isoforms.** We tested the association between the risk alleles rs2287987 (correcting for rs1057569) and rs10044354 (correcting for rs2248374) with 4 detected transcripts at 5q15 in 360 lymphoid cell lines from European ancestry of the 1000 genomes project [27]. The incidence rate ratio (IRR) is calculated as the exponentiated genotype coefficient from the generalized linear mixed model and represents the change in transcript expression (scaled counts) associated with each sequential increase in risk allele count [31]. The IRR^2 is conceptually similar to the change in expression in homozygous risk individuals relative to those homozygous for the protective allele (e.g. 1.542 ~ 54% increase) as previously described [31]. The mean count per transcript is indicated for individuals homozygous for the protective and risk allele. The *P* values are corrected for multiple testing using Bonferroni's correction. Observations of IRR^2 <0.60 or >1.30 (i.e. >30% change in expression) are considered biologically relevant and are highlighted in orange (increase) and blue (decrease).

References

1. McGonagle D, Aydin SZ, Gül A, Mahr A, Direskeneli H. (2015) 'MHC-I-opathy'-unified concept for spondyloarthritis and Behçet disease. Nat Rev Rheumatol. 11:731-40.

2. Kirino Y, et al. (2013) Genome-wide association analysis identifies new susceptibility loci for Behçet's disease and epistasis between HLA-B*51 and ERAP1. Nat Genet. 45:202-7.

3. Cortes A, et al. (2015) Major histocompatibility complex associations of ankylosing spondylitis are complex and involve further epistasis with ERAP1. Nat Commun. 6:7146.

4. Evans D, et al. (2011) Interaction between ERAP1 and HLA-B27 in ankylosing spondylitis implicates peptide handling in the mechanism for HLA-B27 in disease susceptibility. Nat Genet. 43:761-7.

5. Tang H, et al. (2014) A large-scale screen for coding variants predisposing to psoriasis. Nat Genet. 46:45-50.

6. Giza M, Koftori D, Chen L, Bowness P. (2018) Is Behçet's disease a 'class 1-opathy'? The role of HLA-B*51 in the pathogenesis of Behçet's disease. Clin Exp Immunol. 191:11-18.

7. Yazici H, Seyahi E, Hatemi G, Yazici Y. (2018) Behçet syndrome: a contemporary view. Nat Rev Rheumatol. 14:107-119.

8. López de Castro JA, et al. (2016) Molecular and pathogenic effects of endoplasmic reticulum aminopeptidases ERAP1 and ERAP2 in MHC-I-associated inflammatory disorders: Towards a unifying view. Mol Immunol. 77:193-204.

9. Andrés A, et al. (2010) Balancing selection maintains a form of ERAP2 that undergoes nonsense-mediated decay and affects antigen presentation. PLoS Genet. 6:e1001157

10. Reeves E, Edwards CJ, Elliott T, James E. (2013) Naturally occurring ERAP1 haplotypes encode functionally distinct alleles with fine substrate specificity. J Immunol. 19135-43.

11. Takeuchi M, et al. (2016) A single endoplasmic reticulum aminopeptidase-1 protein allotype is a strong risk factor for Behçet's disease in HLA-B*51 carriers. Ann Rheum Dis. 75:2208-2211.

12. Roberts AR, et al. (2017) ERAP1 association with ankylosing spondylitis is attributable to common genotypes rather than rare haplotype combinations. Proc Natl Acad Sci U S 114:558-561.

13. Minos E, et al. (2016) Birdshot chorioretinopathy: current knowledge and new concepts in pathophysiology, diagnosis, monitoring and treatment. Orphanet J Rare Dis. 11:61

14. Shah KH, et al. (2005) Birdshot chorioretinopathy. Surv Ophthalmol. 50:519-41.

15. Yang P, Foster CS. (2013) Interleukin 21, interleukin 23, and transforming growth factor β1 in HLA-A29-associated birdshot retinochoroidopathy. Am J Ophthalmol. 156:400-406.e2.

16. Molins B, Mesquida M, Llorenç V, Sainz de la Maza M, Adán A. (2016) Elevated Serum Immune Mediators and Subclinical Inflammation in HLA-A29-associated Birdshot Chorioretinopathy. Ocul Immunol Inflamm. 24:647-652.

17. Kuiper JJ, Mutis T, de Jager W, de Groot-Mijnes JD, Rothova A. (2011) Intraocular interleukin-17 and proinflammatory cytokines in HLA-A29-associated birdshot chorioretinopathy. Am J Ophthalmol. 152:177-182.e1.

18. Kuiper J, Rothova A, de Boer J, Radstake T. (2015) The immunopathogenesis of birdshot chorioretinopathy; a bird of many feathers. Prog Retin Eye Res. 44:99-110.

19. Herbort CP Jr, et al. (2017) Why birdshot retinochoroiditis should rather be called 'HLA-A29 uveitis'? Br J Ophthalmol. 101:851-855.

20. Kuiper JJ, et al. (2014) A genome-wide association study identifies a functional ERAP2 haplotype associated with birdshot chorioretinopathy. Hum Mol Genet. 23:6081-7.

21. Genome of the Netherlands Consortium. (2014) Whole-genome sequence variation, population structure and demographic history of the Dutch population. Nat Genet. 46:818-25.

22. 1000 Genomes Project Consortium. (2015) A global reference for human genetic variation. Nature. 526:68-74.

23. Purcell S, et al. (2007) PLINK: a tool set for whole-genome association and population-based linkage analyses. Am J Hum Genet. 81:559-75.

24. Márquez A, et al. (2017) New insights into the genetic component of non-infectious uveitis through an Immunochip strategy. J Med Genet. 54:38-46.

25. Evangelou E, Ioannidis JP. (2013) Meta-analysis methods for genome-wide association studies and beyond. Nat Rev Genet. 14:379-89.

26. Delaneau O, Marchini J, Zagury JF. (2011) A linear complexity phasing method for thousands of genomes. Nat Methods. 9:179-81.

27. Lappalainen T, et al. (2013) Transcriptome and genome sequencing uncovers functional variation in humans. Nature. 501:506-11.

28. Collado-Torres L, et al. (2017) Reproducible RNA-seq analysis using recount2. Nat Biotechnol. 35:319-321.

29. Zerbino DR, et al. (2017) Ensembl 2018. Nucleic Acids Res. 46:D754-D761

30. Bates D, Mächler M, Bolker B, Walker S. (2015) Fitting Linear Mixed-Effects Models Using lme4. J Stat Softw. 67.

31. Hanson AL, et al. (2018) Genetic Variants in ERAP1 and ERAP2 Associated With Immune-Mediated Diseases Influence Protein Expression and the Isoform Profile. Arthritis Rheumatol. 70:255-265

32. GTEx Consortium. (2017) Genetic effects on gene expression across human tissues. Nature.550:204-213.

33. Fruci D, et al. (2006) Expression of endoplasmic reticulum aminopeptidases in EBV-B cell lines from healthy donors and in leukemia/lymphoma, carcinoma, and melanoma cell lines. J Immunol. 176:4869-79.

34. Ombrello MJ, Kastner DL, Remmers EF. (2015) Endoplasmic reticulum-associated amino-peptidase 1 and rheumatic disease: genetics. Curr Opin Rheumatol. 27:349-56.

35. Skol AD, Scott LJ, Abecasis GR, Boehnke M. (2006) Joint analysis is more efficient than replication-based analysis for two-stage genome-wide association studies. Nat Genet. 38:209-13.

36. Saveanu L, et al.(2005) Concerted peptide trimming by human ERAP1 and ERAP2 aminopeptidase complexes in the endoplasmic reticulum. Nat Immunol. 6:689-97.

37. Reeves E, Colebatch-Bourn A, Elliott T, Edwards CJ, James E. (2014) Functionally distinct ERAP1 allotype combinations distinguish individuals with Ankylosing Spondylitis. Proc Natl Acad Sci U S A. 111:17594-9.

38. Seregin SS, et al. (2013) Endoplasmic reticulum aminopeptidase-1 alleles associated with increased risk of ankylosing spondylitis reduce HLA-B27 mediated presentation of multiple antigens. Autoimmunity. 46:497-508.

39. Guasp P, et al. (2017) The Behçet's disease-associated variant of the aminopeptidase ERAP1 shapes a low-affinity HLA-B*51 peptidome by differential subpeptidome processing. J Biol Chem. 292:9680-9689.

40. Robinson PC, et al. (2015) ERAP2 is associated with ankylosing spondylitis in HLA-B27-positive and HLA-B27-negative patients. Ann Rheum Dis. 74:1627-9.

41. Mpakali A, et al. (2017) Crystal Structures of ERAP2 Complexed with Inhibitors Reveal Pharmacophore Requirements for Optimizing Inhibitor Potency. ACS Med Chem Lett. 8:333-337.

    Mpakali A, et al. (2015) Structural Basis for Antigenic Peptide Recognition and Processing by Endoplasmic Reticulum (ER) Aminopeptidase 2. J Biol Chem. 290:26021-32

42. Levinson RD, et al. (2008) Combination of KIR and HLA gene variants augments the risk of developing birdshot chorioretinopathy in HLA-A*29-positive individuals. Genes Immun. 9:249-58.

43. Robinson PC, et al. (2016) The genetic associations of acute anterior uveitis and their overlap with the genetics of ankylosing spondylitis. Genes Immun. 17:46-51.

44. Alvarez-Navarro C, Martín-Esteban A, Barnea E, Admon A, López de Castro JA. (2015) Endoplasmic Reticulum Aminopeptidase 1 (ERAP1) Polymorphism Relevant to Inflammatory Disease Shapes the Peptidome of the Birdshot chorioretinopathy-Associated HLA-A*29:02 Antigen. Mol Cell Proteomics. 14:1770-80.

45. Chen H, Li L, Weimershaus M, Evnouchidou I, van Endert P, Bouvier M. (2016) ERAP1-ERAP2 dimers trim MHC I-bound precursor peptides; implications for understanding peptide editing. Sci Rep. 12:28902.

46. Martín-Esteban A, et al. (2017) Separate effects of the ankylosing spondylitis associated ERAP1 and ERAP2 aminopeptidases determine the influence of their combined phenotype on the HLA-B*27 peptidome. J Autoimmun. 79:28-38.

47. Nossent JC, Johnsen S, Bakland G. (2016) The influence of ERAP1 gene variants on clinical phenotype in ankylosing spondylitis. Scand J Rheumatol. 45:474-479.

48. Masouri S, et al. (2016) A Pharmacogenetic Study of Psoriasis Risk Variants in a Greek Population and Prediction of Responses to Anti-TNF-α and Anti-IL-12/23 Agents. Mol Diagn Ther. 20:221-5.

49. Ozen G, et al. (2017) Association of ERAP1, IL23R and PTGER4 Polymorphisms with Radiographic Severity of Ankylosing Spondylitis. Open Rheumatol J. 16:1-9.

50. Baeten D, et al. (2013) Anti-interleukin-17A monoclonal antibody secukinumab in treatment of ankylosing spondylitis: a randomised, double-blind, placebo-controlled trial. Lancet 382:1705–13

51. Georgiadis D, Mpakali A, Koumantou D, Stratikos E. (2018) Inhibitors of ER aminopeptidase 1 and 2: from design to clinical application. Curr Med Chem. 2018 Feb 13.

52. Pruim RJ, et al. (2010) LocusZoom: regional visualization of genome-wide association scan results. Bioinformatics. 26:2336-7

Figure 1

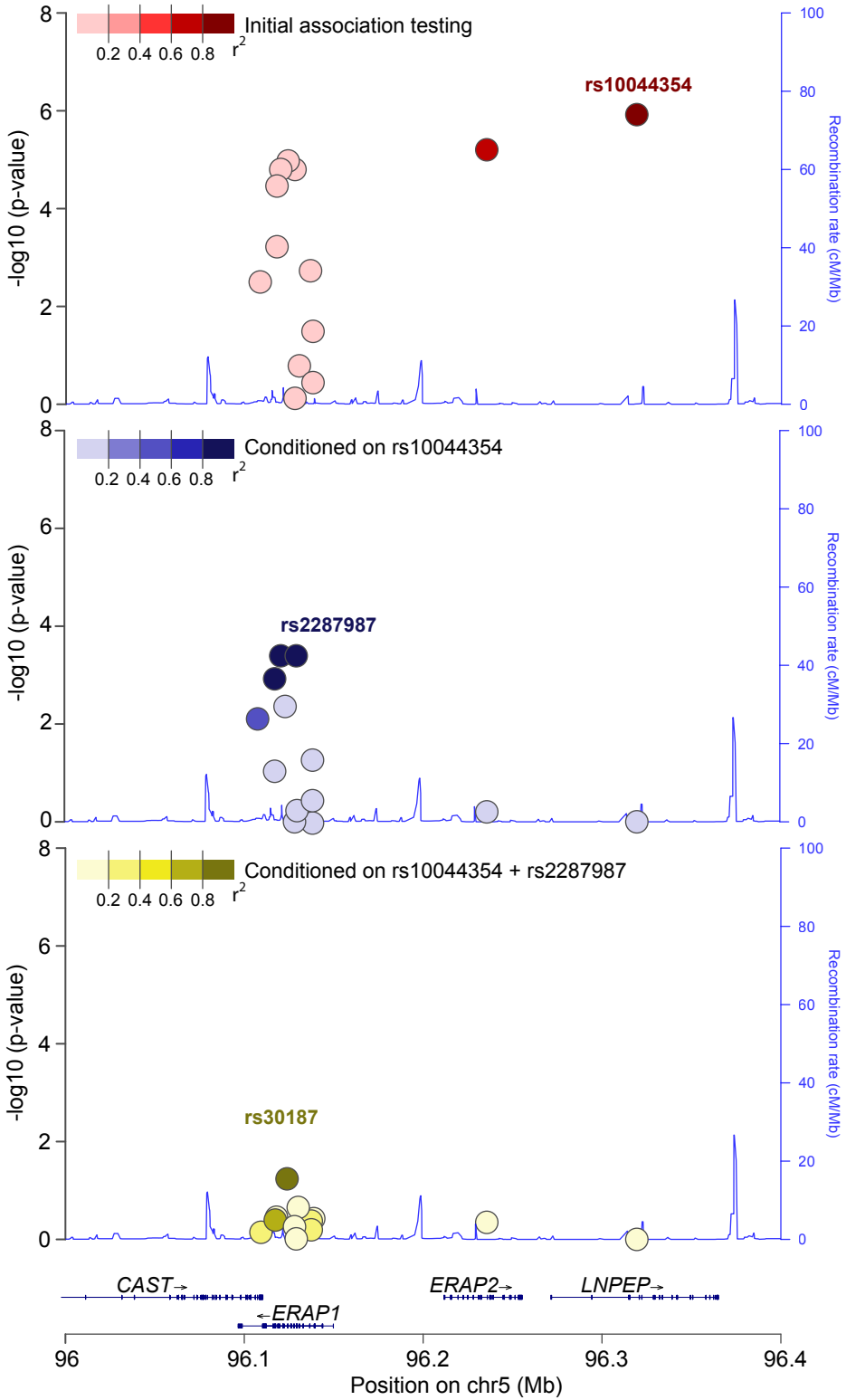
Initial association testing
0.2 0.4 0.6 0.8
r2
rs10044354
-log10 (p-value)
Recombination rate (cM/Mb)
Conditioned on rs10044354
rs2287987
Conditioned on rs10044354 + rs2287987
rs30187
CAST
ERAP2
LNPEP
ERAP1
96
96.1
96.2
96.3
96.4
Position on chr5 (Mb)

Figure 2

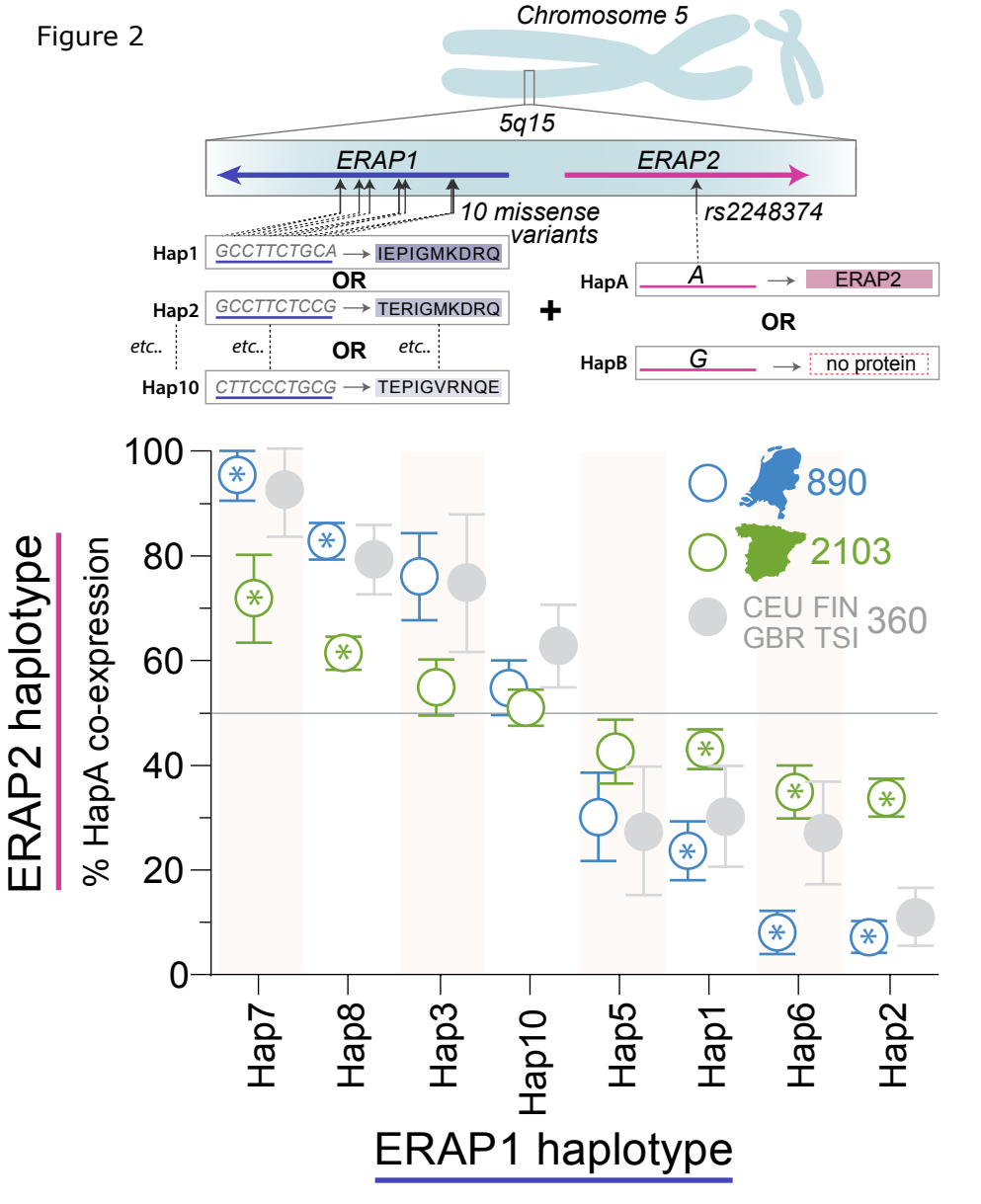
Chromosome 5
5q15
ERAP1
ERAP2
10 missense variants
rs2248374
Hap1
GCCTTCTGCA
IEPIGMKDRQ
OR
Hap2
GCCTTCTCCG
TERIGMKDRQ
etc..
etc..
OR
etc..
Hap10
CTTCCCTGCG
TEPIGVRNQE
+
HapA
A
ERAP2
OR
HapB
G
no protein
ERAP2 haplotype
% HapA co-expression
100
80
60
40
20
0
890
2103
CEU FIN
GBR TSI
360
Hap7
Hap8
Hap3
Hap10
Hap5
Hap1
Hap6
Hap2
ERAP1 haplotype

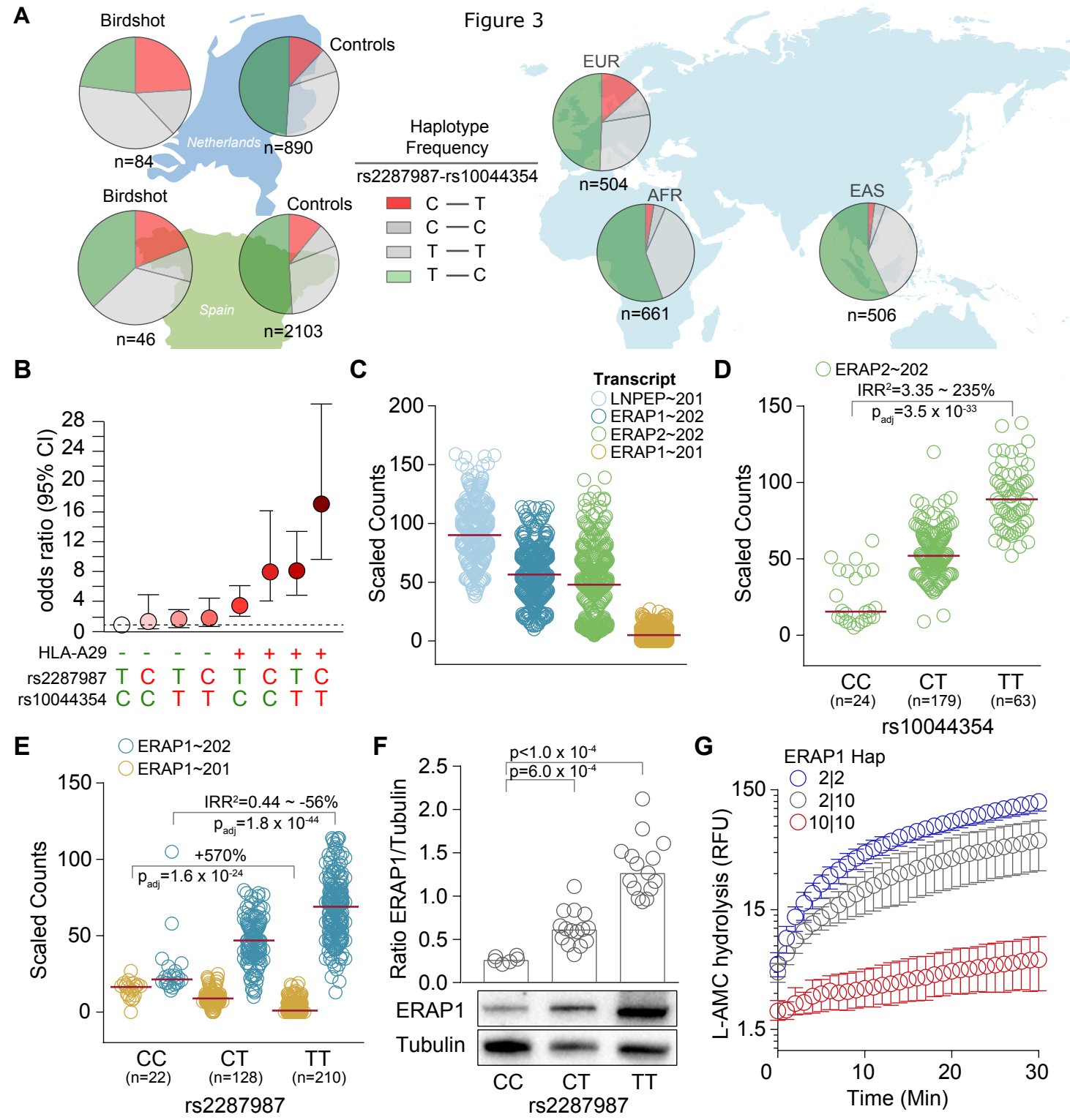
Figure 3
A
Birdshot
Controls
Netherlands
n=84
n=890
Birdshot
Controls
Spain
n=46
n=2103
Haplotype Frequency
rs2287987-rs10044354
C — T
C — C
T — T
T — C
EUR
n=504
AFR
n=661
EAS
n=506
B
odds ratio (95% CI)
HLA-A29
rs2287987
rs10044354
C
Transcript
LNPEP~201
ERAP1~202
ERAP2~202
ERAP1~201
Scaled Counts
D
ERAP2~202
IRR²=3.35 ~ 235%
p_adj=3.5 x 10^-33
Scaled Counts
CC (n=24)
CT (n=179)
TT (n=63)
rs10044354
E
ERAP1~202
ERAP1~201
IRR²=0.44 ~ -56%
p_adj=1.8 x 10^-44
+570%
p_adj=1.6 x 10^-24
Scaled Counts
CC (n=22)
CT (n=128)
TT (n=210)
rs2287987
F
p<1.0 x 10^-4
p=6.0 x 10^-4
Ratio ERAP1/Tubulin
ERAP1
Tubulin
CC
CT
TT
rs2287987
G
ERAP1 Hap
2|2
2|10
10|10
L-AMC hydrolysis (RFU)
Time (Min)

Supplementary info for:

Functionally distinct ERAP1 and ERAP2 are a hallmark of HLA-A29-(Birdshot) Uveitis.

J.J.W. Kuiper et al.

Included here are:
Supplementary Figures
Supplementary Tables

Supplementary Figures

Supplementary Figure 1 | Analysis of genetic matching of cases and controls. Principle component analysis (PCA)first versus second and second versus third component in cases and controls using genotype data from the Dutch collections as described in method section. PCA was computed using a set of random 75,239 independent SNPs autosome-wide (chr 1-22) in EIGENSOFT (*Price et al. Principal components analysis corrects for stratification in genome-wide association studies. Nat Genet. 2006 Aug;38(8):904-9*), excluding the *MHC*, two large inversions on chromosomes 8 and 17 and the *LCT* locus on chromosome 2. The SNPs all had a minor allele frequency (MAF) <0.1, were not in Hardy-Weinberg equilibrium ($p < 10^{-4}$) and showed a pairwise LD of 0.2 or less.

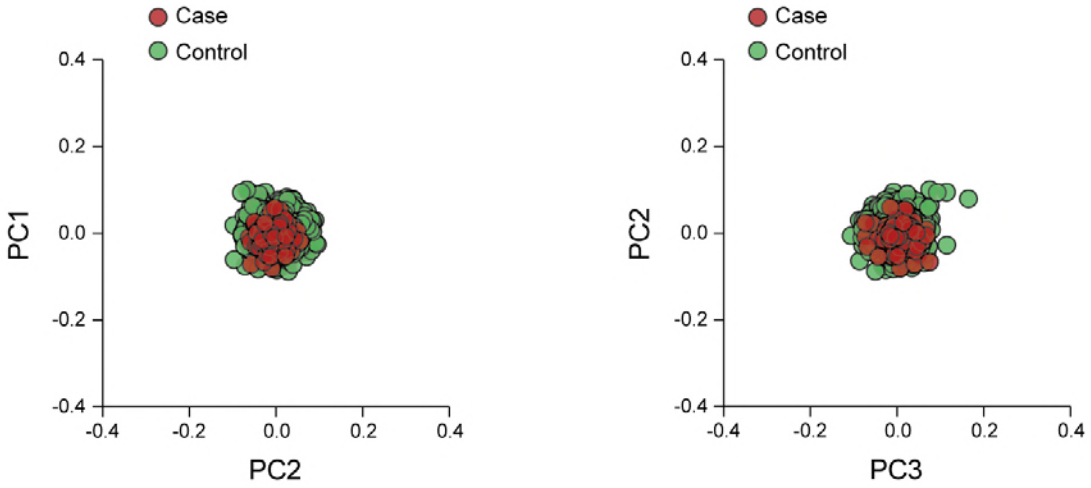

Supplementary Figure 2 | Three-dimensional surface model for the ERAP1 allotype associated with Birdshot uveitis (Protein Data Bank entry: 3MDJ). Common variant amino acid residues in ERAP1 are displayed as spheres; Ancestral amino acids are highlighted in green and non-ancestral amino acid positions are highlighted in red. 3D structure was produced using UCSF Chimera (*Pettersen, E. F. et al. UCSF Chimera - a visualization system for exploratory research and analysis. J. Comput. Chem. 25, 1605–1612 2004*).

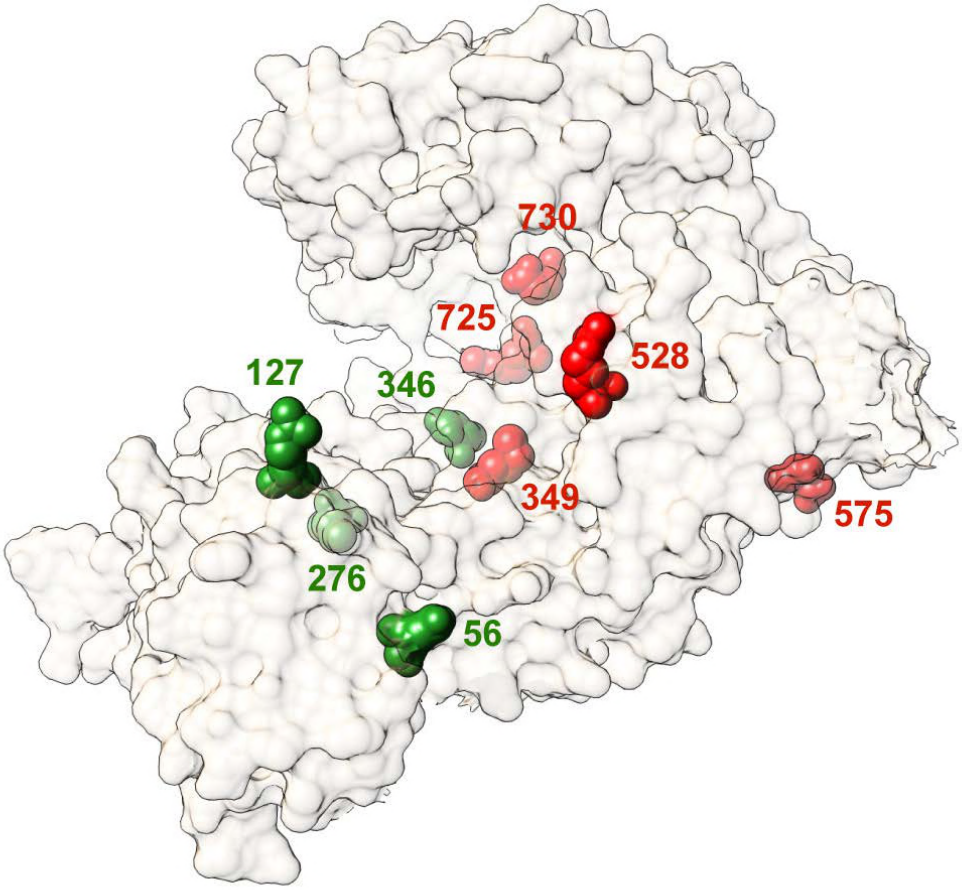

Supplementary Figure 3 The estimated haplotype frequency (%) for the 8 common ERAP1 haplotypes using Plink and SHAPEIT for cases (in red) and controls (in green). The dotted diagonal line indicates perfect correlation between the estimated haplotype frequencies.

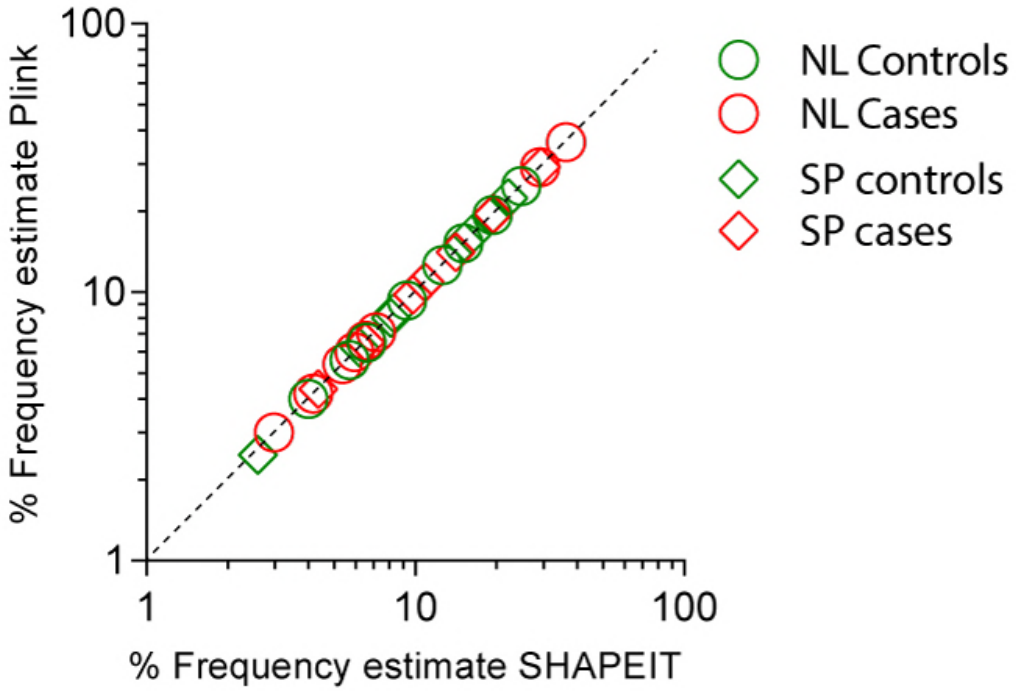

Supplementary Figure 4 | ERAP1 and ERAP2 expression in B cell lines of Birdshot uveitis and HLA-A29-positive controls. We assessed ERAP1 and ERAP2 protein levels in EBV transformed B cells (EBV-LCL), from twelve HLA-A*2902-positive individuals (except NA11994) from the 1000 Genomes project and EBV-LCLs generated from peripheral blood mononuclear cells of four BU patients genotyped in this study, by western blotting. Protein lysates (10µg/lane) from cells were separated on a 4-20% Mini-PROTEAN TGX gel (Bio-Rad Laboratories) and transferred to a PVDF membrane. Proteins were detected using a 1:5000 dilution of primary antibodies; goat anti-ERAP2 polyclonal antibody (AF3830, R&D Systems), goat anti-ERAP1 polyclonal antibody (AF2334, R&D Systems) and anti-α-tubulin monoclonal prepared in mouse (T6199, Sigma). Anti-mouse secondary antibody conjugated to Horseradish Peroxidase (HRP) (Jackson ImmunoResearch; 1:5000) and anti-goat secondary antibody conjugated to HRP (DAKO; 1:5000) were used to probe primary antibodies. Protein bands were detected with Amersham Prima Western Blotting (RPN22361, GE Healthcare) on the ChemiDoc Gel Imaging System (Bio-Rad Laboratories). Independent experiments are individually outlined below for ERAP1. The ratio of the intensity of the ERAP1 over α-tubulin band was calculated using Image Lab 5.1 (Bio-Rad Laboratories) for each experiment. All ratios of the intensities were grouped according to the distribution of *Hap10* (red = homozygous for rs2287987-C, orange = heterozygous for rs2287987-C, green is non-carriers) for quantitative analysis as outlined in **Figure 3F**.

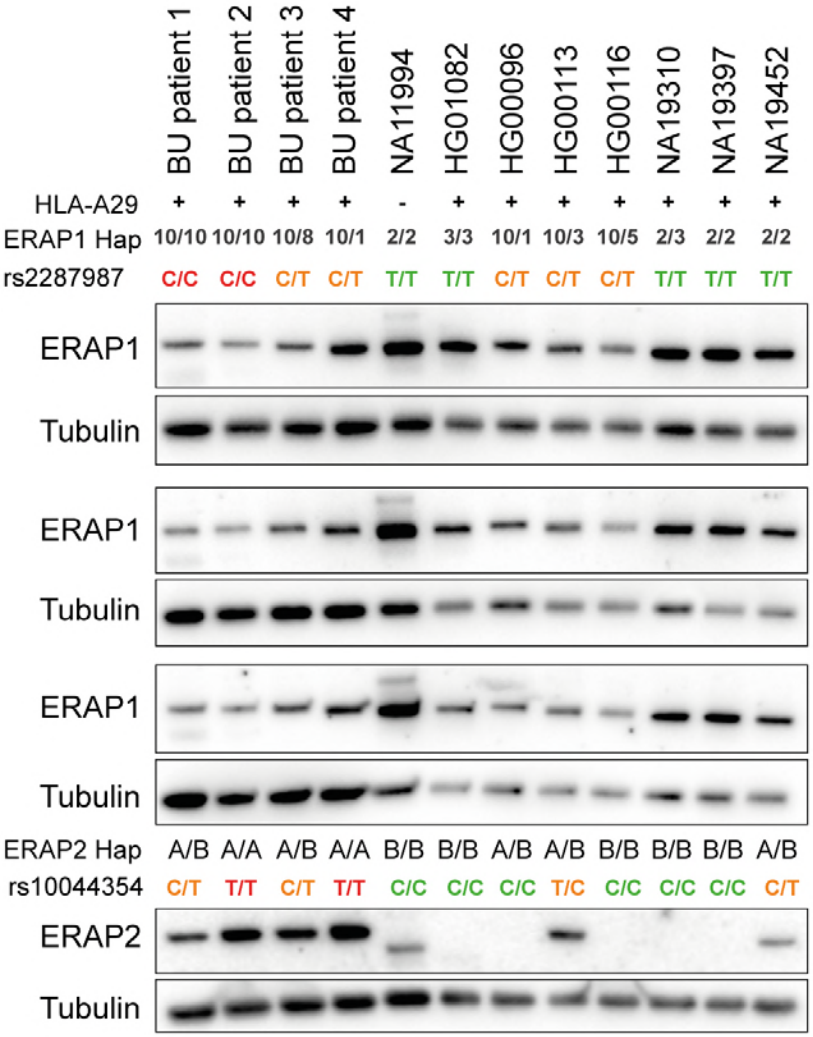

Supplementary Figure 5 | rs10044354 is in tight LD with a splice region variant in LNPEP. We searched the 5 European populations (British [GBR], Iberian [IBS], Finnish [FIN], Utah residents with Northern and Western European Ancestry [CEU], and Tuscany [TSI]) of the *1000 Genomes Project* for missense or splice region variants of *LNPEP* in high LD (r^2 >0.75) with rs10044354; The rs10044354 variant is in tight LD (r^2 >0.96-1.0) with rs3836862 located in the splice region of intron 6-7 of *LNPEP*. These exons encode the key Zn-binding motif of the enzyme. The *Human splicing finder* software (http://www.umd.be/HSF3/) predicted a potential impact of the rs3836862 on splicing of this region. To explore if rs3836862 altered splicing of intron-6-7, we tested if the presence of rs10044354/rs3836862 affects the sequence of the predominant mature transcripts near this splice region. We selected four lymphoid cell lines that were homozygous null and four homozygous carries of the C allele of rs3836862 (as determined by Sanger sequencing). For each cell line, a total of 1 × 10^6 cells were cultured in 2 mL RPMI 1640 (Life Technologies), supplemented with 10% (v/v) heat-inactivated FCS (Biowest) and 1% (v/v) penicillin and streptomycin (Life Technologies) in a six wells plate for 24 hours and stimulated with TLR agonists resiquimod (*R848*; 1 µg/ml), or CpG-B (*ODN684*; 5 µM, both from *InvivoGen*), or left untreated. Total RNA was extracted using QiaCube and RNeasy mini kit (*Qiagen*) and a 443 bp cDNA fragment from exon 5 to exon 8 of *LNPEP* was generated by SuperScript ® cDNA synthesis kit (Invitrogen, UK) using 5'-3' (forward) TATGCCTTGGAAACAACTGTGA and 5'-3'(reverse) TGTTCTGAAGACTGAACAGA TGAT. A 438 bp cDNA fragment was amplified using proof reading Pfu DNA polymerase-PCR reaction (Agilent Technologies, Santa Clara, CA, USA) with 5'-3'(forward) TGCCTTGGAAA CAACTGTGAAG and 5'-3' (reverse) TCTGAAGACTGAACAGATGATGA. A single band was detected in all conditions by agarose gel and sequenced at Macrogen Europe (Netherland) with 5'-3'(forward) GGAAACAACTGTGAAGCTTCTTGA and 5'-3'(reverse) CTTTCTTCATGGTTTT AAATCGAGC. Chromatograms from representative donors (unstimulated) from each group are indicated below. These analyses detected a sequence identical to the canonical transcript of *LNPEP* (Ensemble ID *ENST00000231368*) in all samples. We concluded that rs3836862 does not affect the sequence of the predominant (detectable) mature LNPEP transcripts in lymphoid cell lines under the described conditions.

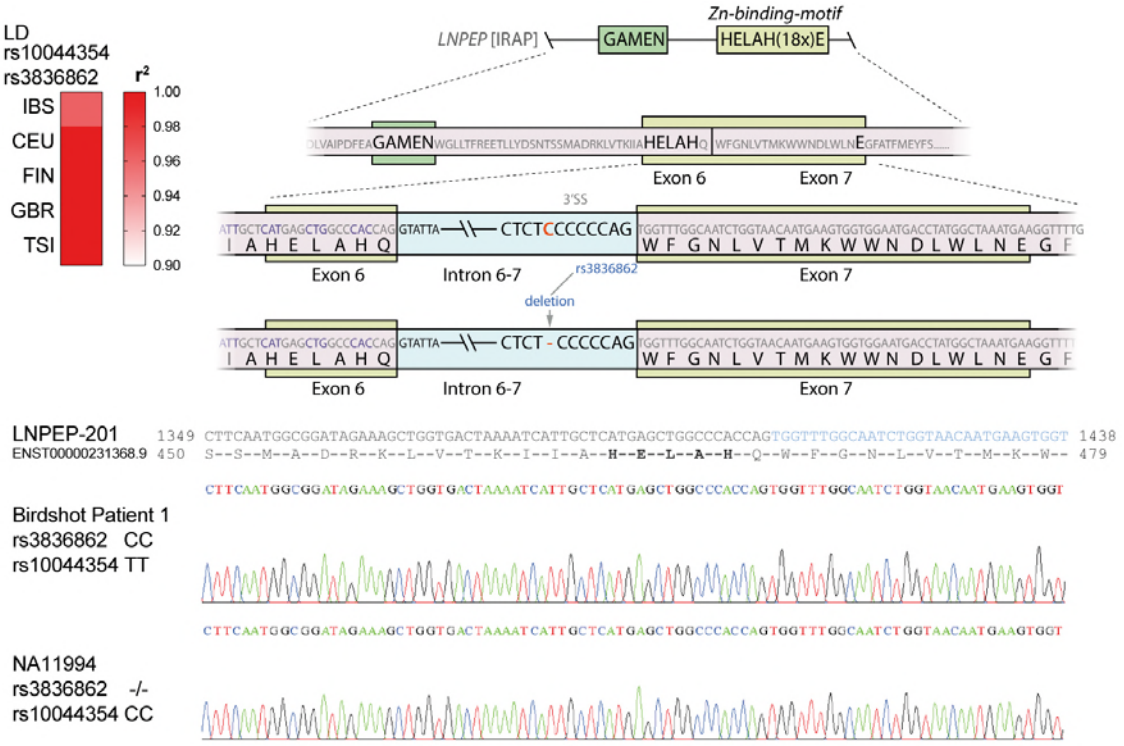

Supplementary Figure 6 | The common splice region variant of *ERAP2* tags the bimodal distribution of protein expression. *ERAP2* encodes at least two common haplotypes that are tagged by rs2248374. The A allele tags the protein-coding haplotype (HapA), while the G allele tags a haplotype that encodes a transcript that is usually prone to none-sense mediated decay [9] and loss strongly reduced protein expression. Expression of ERAP2 in CEPH controls according to rs2248374 genotype is provided for three B-cell lines from individuals from the CEPH panel (*Dausset J. et al. Centre d'etude du polymorphisme humain (CEPH): collaborative genetic mapping of the human genome. Genomics. 1990;6:575–577*). Genotype information was obtained from the *Ensembl Genome Browser* (rs2248374 or rs2549797 that is in full LD [r^2 =1] with rs2248374). Cells were lysed and ERAP2 expression was assessed after SDS–PAGE and western blotting with antibodies to ERAP2. The endogenous levels of β-tubulin protein were analyzed as a loading control.

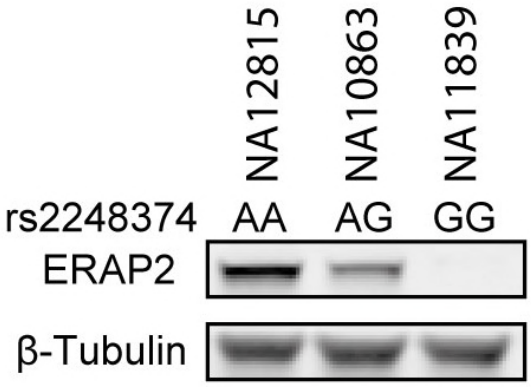

Supplementary Figure 7 | Linkage disequilibrium across the 13 polymorphisms in *ERAP1* and *ERAP2* in cases and controls. **Left**: The linkage disequilibrium across the functional variants at 5q15. The heatmaps show the D'prime and r^2 values calculated for SNPs in the Dutch and Spanish controls.

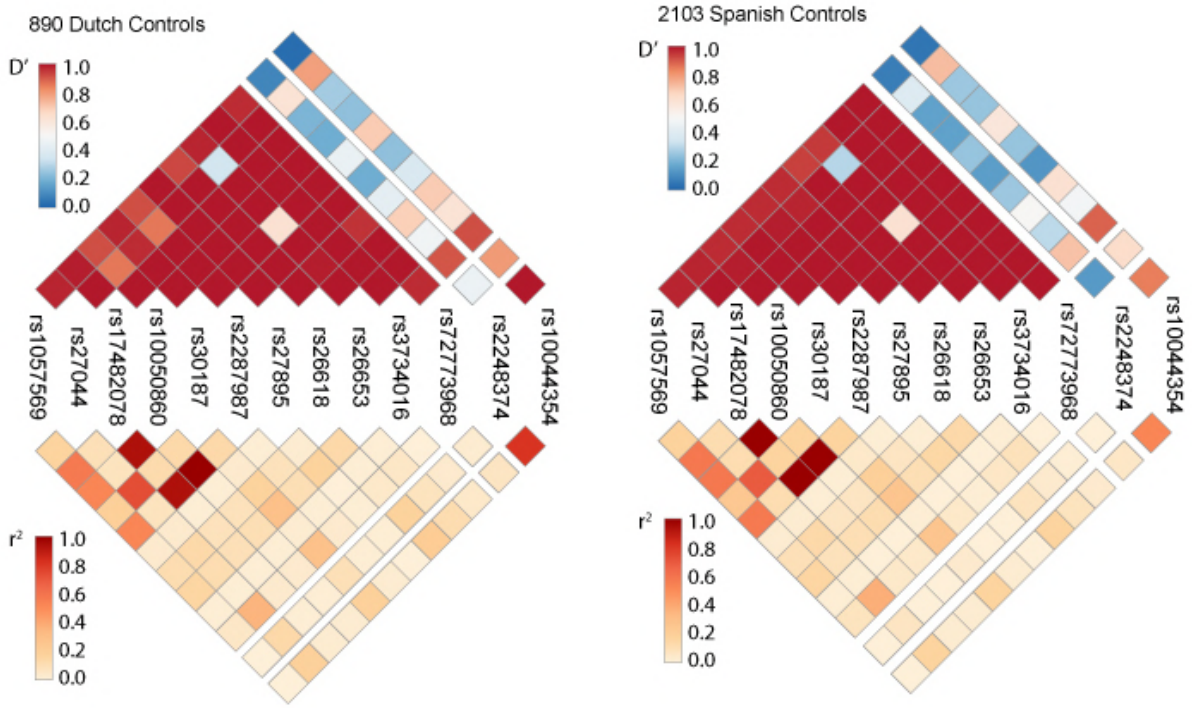

Supplementary Figure 8 | Non-random distribution of the ERAP2-protein coding haplotype across common ERAP1 haplotypes based on 5 SNPs. Five missense variants in *ERAP1* encode four discrete and common (>1% freq) haplotypes [12], while *ERAP2* encodes 1 common protein-coding haplotype (*HapA* tagged by the A allele of rs2248374) and non-coding haplotypes (tagged by the G allele). Each chromosome harbors 1 ERAP1 haplotype and 1 ERAP2 haplotype. We outlined the percentage of *HapA* per ERAP1 haplotype on the same chromosome using phased ERAP1-ERAP2 haplotype data of 890 Dutch controls (blue) and ERAP1-ERAP2 haplotype data for the 360 samples from the CEU, FIN, GBR, and TSI populations (grey) from the 1000 Genomes sample collection used for functional investigation in this study [27].

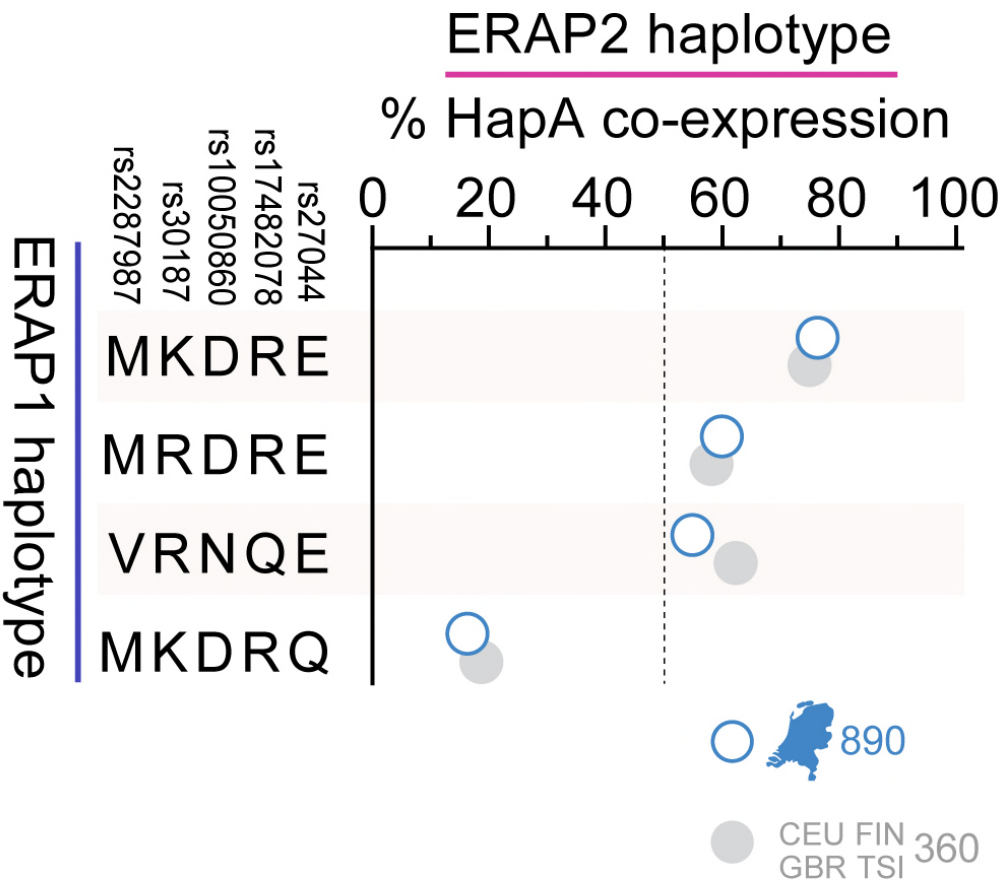

Supplementary Figure 9 | The normalized effect size from the eQTL analysis for variants at 5q15 derived from the Genotype-Tissue Expression (GTEx) Project. Data for 117 lymphoid cell lines and 369 whole blood samples were obtained from the GTExportal (GTEx Analysis Release V7) as described in the method section.

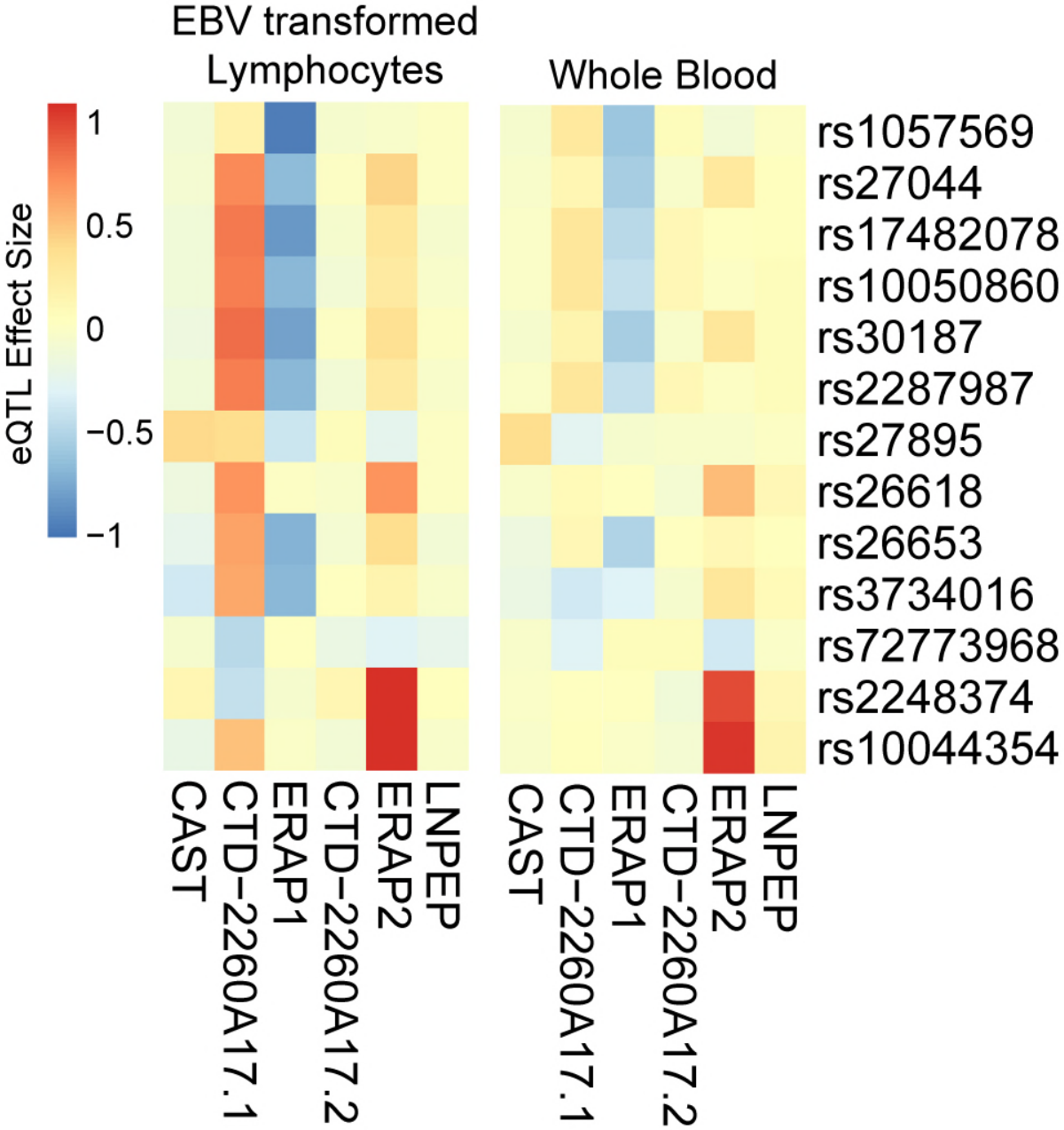

Supplementary Figure 10 | eQTL data for variants in *ERAP1* and *ERAP2* in lymphoid cell lines of 117 individuals from the Genotype-Tissue Expression (GTEx) Project. P values from eQTL analysis for *ERAP1* and *ERAP2* were obtained from the Genotype-Tissue Expression (GTEx) [32] Project (GTEx Analysis Release V7). The eQTLs for ERAP1 and ERAP2 identified in this study are indicated. Hg19 EUR 2014 1000 genomes LD structure. Plots were generated in LocusZoom [52].

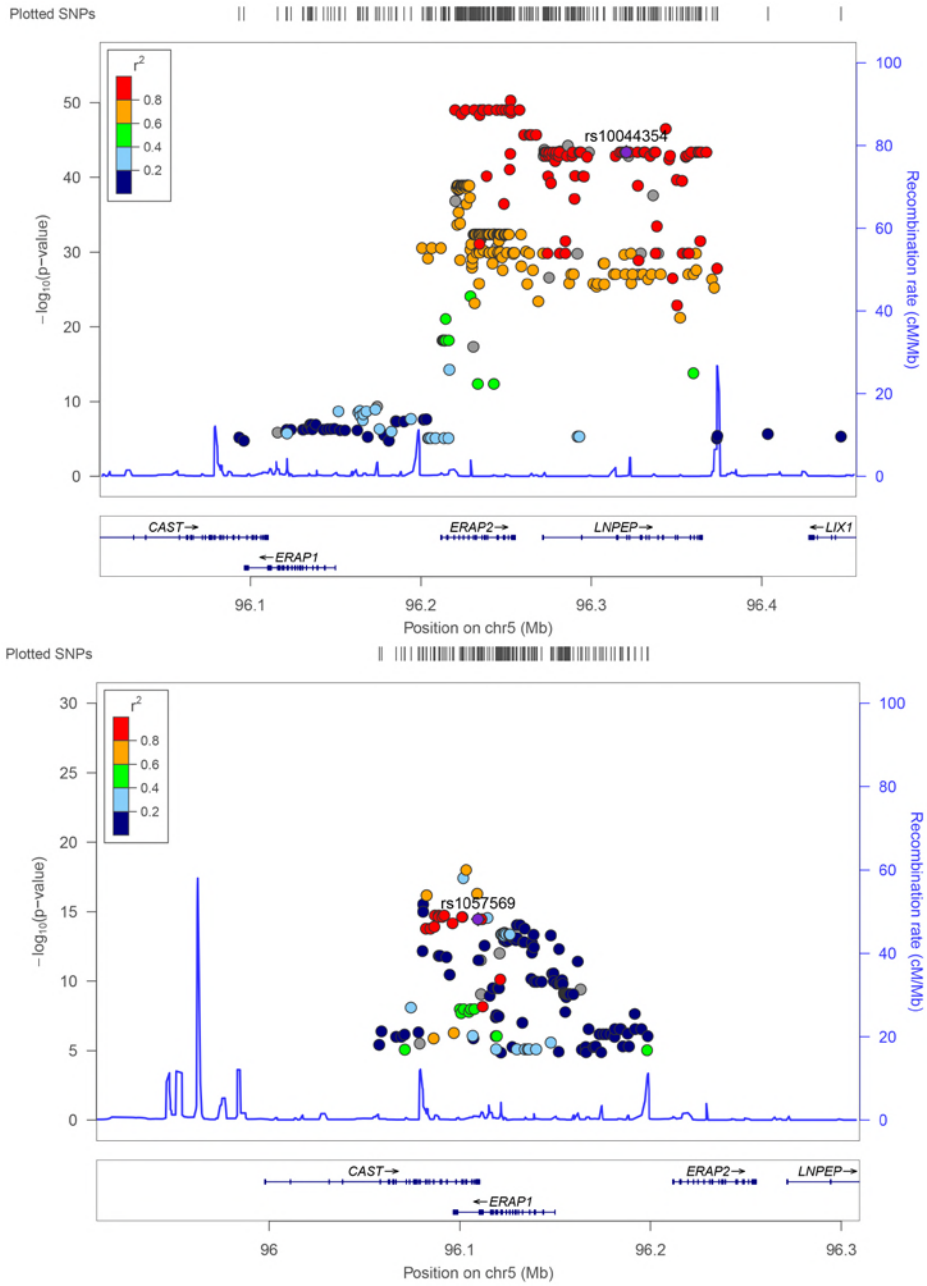

Supplementary Tables

Supplementary Table 1. Association results for common functional variants at 5q15 in *ERAP1*, *ERAP2* and *LNPEP* genes in Dutch and Spanish populations.

CHR	Gene	Function	SNP	Position	Allele (minus strand)	*Netherlands*				*Spain*				*Meta -analysis*	
						Freq		OR (95% CI)	*P*	Freq		OR (95% CI)	*P*		
						Case (n=84)	Control (n=890)			Case (n=46)	Control (n=2103)			*OR*	*P*
5	*ERAP1*	eQTL of *ERAP1*	rs1057569	96109610	A	0.42	0.29	1.69(1.19-2.40)	3.25×10^{-3}	0.35	0.28	1.37(0.89-2.11)	0.15	1.56	1.41×10^{-3}
5	*ERAP1*	730Q	rs27044	96118852	G	0.15	0.29	0.45(0.29-0.71)	5.84×10^{-4}	0.24	0.32	0.67(0.42-1.08)	0.10	0.55	2.89×10^{-4}
5	*ERAP1*	725Q	rs17482078	96118866	T	0.36	0.19	2.20(1.51-3.20)	3.53×10^{-5}	0.29	0.19	1.73(1.10-2.71)	0.017	1.99	2.58×10^{-6}
5	*ERAP1*	575N	rs10050860	96122210	T	0.38	0.21	2.24(1.56-3.24)	1.51×10^{-5}	0.29	0.19	1.70(1.08-2.67)	0.021	2.01	1.46×10^{-6}
5	*ERAP1*	528K	rs30187	96124330	T	0.16	0.34	0.37(0.24-0.58)	1.20×10^{-5}	0.35	0.40	0.80(0.52-1.23)	0.31	0.55	1.53×10^{-4}
5	*ERAP1*	349V	rs2287987	96129535	C	0.38	0.20	2.25(1.56-3.24)	1.49×10^{-5}	0.29	0.19	1.70(1.09-2.67)	0.020	2.01	1.41×10^{-6}
5	*ERAP1*	346D	rs27895	96129543	T	0.07	0.07	0.92(0.47-1.81)	0.82	0.05	0.06	0.86(0.35-2.11)	0.75	0.90	0.70
5	*ERAP1*	276M	rs26618	96130836	C	0.29	0.25	1.32(0.90-1.92)	0.16	0.20	0.22	0.85(0.51-1.42)	0.53	1.13	0.45
5	*ERAP1*	127R	rs26653	96139250	C	0.17	0.28	0.50(0.33-0.78)	1.87×10^{-3}	0.25	0.31	0.74(0.46-1.18)	0.20	0.60	2.00×10^{-3}
5	*ERAP1*	56K	rs3734016	96139464	T	0.05	0.04	1.42(0.68-2.95)	0.35	0.04	0.03	1.69(0.62-4.58)	0.31	1.51	0.18
5	*ERAP1*	12I	rs72773968	96139595	A	0.06	0.13	0.48(0.24-0.94)	0.03	0.14	0.15	0.90(0.50-1.61)	0.72	0.69	0.09
5	*ERAP2*	Splice-variant	rs2248374	96235896	A	0.67	0.47	2.26(1.59-3.22)	6.11×10^{-6}	0.56	0.48	1.40(0.92-2.12)	0.12	1.85	7.96×10^{-6}
5	*LNPEP*	eQTL of *ERAP2*	rs10044354	96320495	T	0.63	0.42	2.42(1.69-3.45)	1.21×10^{-6}	0.53	0.40	1.68(1.11-2.55)	0.014	2.07	1.24×10^{-7}

Supplementary Table 2 | Distribution of Hap10 in the Dutch and Spanish cases and controls. The frequency of the rs2287987-C (i.e. Hap10+ individuals) or rs2287987-CC (i.e. Hap10 homozygous individuals) genotypes in cases and controls was tested by Fischer's exact test. OR; odds ratio. 95%CI; 95% confidence interval.

Cohort	% of individuals with rs2287987 CT+CC genotype		OR (95%CI)	*P* value	% of individuals with rs2287987 CC genotype		OR (95%CI)	*P* value Fischer's Exact test
	Case	Control			Case	Control		
	CT+CC	CT+CC			CC	CC		
Netherlands	63.1	37.2	2.88(1.78-4.75)	6.34×10^{-6}	13.1	3.7	3.90(1.71-8.33)	7.36×10^{-4}
Spain	45.7	34.7	1.58(0.83-2.96)	0.16	13.0	4.1	3.55(1.20-8.74)	0.0118

Supplementary Table 3 | Results of test for association of the haplotype rs2287987 (risk allele C) and rs10044354 (risk allele T) with Birdshot Uveitis in 130 cases and 2993 controls using a logistic regression model.

Cohort	rs2287987	rs10044354	Haplotype Frequency		OR	P value
			Cases	Controls		
Netherlands	C	T	0.24	0.12	3.1	1.4×10^{-6}
	T	T	0.39	0.31	1.4	0.05
	C	C	0.14	0.08	1.3	0.33
	T	C	0.23	0.49	0.30	3.5×10^{-8}
Spain	C	T	0.19	0.11	2.3	3.9×10^{-3}
	T	T	0.34	0.30	1.2	0.36
	C	C	0.10	0.08	1.2	0.63
	T	C	0.37	0.51	0.53	6.2×10^{-3}

Supplementary Table 4 | The frequency of the rs2248374 A allele in *ERAP2* co-occurring with each of the 8 common ERAP1 haplotypes is non-random in phased haplotype data of 890 Dutch and 2103 Spanish controls. The *ERAP2* protein-coding haplotype [11] is tagged by the A allele of rs2248374 in *ERAP2*. We used a two-sided exact binominal test to assess if the observed frequencies were non-random (deviation from a test probability of 0.5 or the hypothesis that ERAP2 co-occurs in 50% of any particular ERAP1 haplotype). Frequency distribution of ERAP2 for each of the ERAP1 haplotypes was considered non-random if the frequency deviated at a significant level of [A or G rs2248374 for 8 ERAP1 haplotypes = 0.05/16] $p<2.5 \times 10^{-3}$ in both the Dutch and Spanish populations (with consistent direction of deviation from 50%). ERAP1 haplotypes that fulfilled these criteria are highlighted (in orange haplotypes that more frequently co-occur with rs2248374-A allele and in blue haplotypes that less frequently co-occur with rs2248374-A allele).

ERAP1 haplotype	Number of Dutch haplotypes (n=1780)	% Co-occurring A-rs2248374 (95% CI)	P value	Number of Spanish haplotypes (n=4206)	% Co-occurring A-rs2248374 (95% CI)	P value
*Hap1**	225	24(18-30)	7.35×10^{-16}	641	43(39-47)	3.71×10^{-4}
*Hap2**	268	7(4-11)	2.66×10^{-52}	683	34(30-37)	1.02×10^{-17}
Hap3	101	76(67-84)	1.18×10^{-7}	340	55(49-60)	0.093
Hap5	117	30(22-39)	1.65×10^{-5}	259	42(36-49)	0.018
*Hap6**	165	8(4-13)	3.10×10^{-31}	348	35(30-40)	1.42×10^{-8}
*Hap7**	71	96(88-99)	5.06×10^{-17}	110	72(62-80)	5.34×10^{-6}
*Hap8**	442	83(79-86)	1.41×10^{-46}	935	61(58-64)	5.33×10^{-12}
Hap10	345	55(49-60)	0.085	808	51(47-54)	0.65
Total (% of ERAP1 haplotypes)	**1734 (97%)**			**4124 (98%)**		

***Supplementary Table 5* | Birdshot-associated SNPs are eQTLs for *ERAP1* and *ERAP2* isoforms.** We tested the association between the risk alleles rs2287987 (correcting for rs1057569) and rs10044354 (correcting for rs2248374) with 4 detected transcripts at 5q15 in 360 lymphoid cell lines from European ancestry of the 1000 genomes project [27]. The incidence rate ratio (IRR) is calculated as the exponentiated genotype coefficient from the generalized linear mixed model and represents the change in transcript expression (scaled counts) associated with each sequential increase in risk allele count [31]. The IRR^2 is conceptually similar to the change in expression in homozygous risk individuals relative to those homozygous for the protective allele (e.g. 1.542 ~ 54% increase) as previously described [31]. The mean count per transcript is indicated for individuals homozygous for the protective and risk allele. The *P* values are corrected for multiple testing using Bonferroni's correction. Observations of IRR^2 <0.60 or >1.30 (i.e. >30% change in expression) are considered biologically relevant and are highlighted in orange (increase) and blue (decrease).

	Risk allele	IRR (95%CI)	IRR^2 (95%CI)	% change expression AA x BB	P value	Mean count in homozygous Protective allele	Mean count in homozygous Protective allele	Ratio Risk/Protective AA x BB
ERAP1~201 ENST00000296754.7								
rs1057569	A	4.13(3.63 -4.7)	17.05(13.15-22.1)	1605%	1.66×10^{-100}	1.17	15.78	13.49
rs2287987	C	2.59(2.17 -3.09)	6.7(4.7-9.56)	570%	1.56×10^{-24}	3.18	14.86	4.67
rs2287987 corrected for rs1057569	C	1.03(0.87 -1.21)	1.05(0.76-1.47)	5%	1			
rs10044354 corrected for rs1057569	T	1.01(0.9 -1.13)	1.02(0.82-1.27)	2%	1	5.29	7.22	1.36
ERAP1~202 ENST00000443439.6								
rs1057569	A	0.62(0.59 -0.64)	0.38(0.35-0.42)	-62%	1.93×10^{-105}	74.37	25.36	0.34
rs2287987	C	0.66(0.62 -0.7)	0.44(0.39-0.49)	-56%	1.77×10^{-44}	68.01	27.54	0.40
rs2287987 corrected for rs1057569	C	0.98(0.91 -1.05)	0.96(0.83-1.11)	-4%	1			
rs10044354 corrected for rs1057569	T	0.93(0.9 -0.97)	0.87(0.8-0.94)	-13%	8.06×10^{-3}	64.10	49.61	0.77
ERAP2~202 ENST00000437043.7								
rs1057569 corrected for rs2248374	A	1.07(1 -1.14)	1.14(1.01-1.3)	14%	0.54	57.05	69.31	1.21
rs2287987 corrected for rs2248374	C	1.06(0.99 -1.14)	1.13(0.99-1.29)	13%	1	57.05	72.10	1.26
rs10044354 corrected for rs2248374	T	1.83(1.66 -2.02)	3.35(2.76-4.06)	235%	3.48×10^{-33}	23.75	89.61	3.77
LNPEP~201 ENST00000231368.9								
rs1057569	A	0.99(0.95 -1.03)	0.98(0.9-1.06)	-2%	1	92.22	89.60	0.97
rs2287987	C	0.99(0.94 -1.03)	0.97(0.89-1.06)	-3%	1	91.06	87.86	0.96
rs10044354	T	0.97(0.93 -1.01)	0.94(0.87-1.01)	-6%	1	92.00	87.49	0.95

Supplementary Table 6. ERAP1 Amino Acids positions for Haplotype 10 (Hap10). Using molecular cloning, full-length *ERAP1* was sequenced from a patient homozygous for *Hap10 and a patient heterozygous for Hap10 (based on common genotyped SNPs)*. Previously reported amino acid positions in *ERAP1* are adapted from *Reeves et al.*[37] and *Ombrello et al.* [34]

	Amino Acid position in ERAP1																	
Allotype	**12**[a]	**56**[a,b]	**82**[b]	**102**[b]	**115**[b]	**127**[a,b]	**199**[b]	**276**[a,b]	**346**[a,b]	**349**[a,b]	**528**[a,b]	**575**[a,b]	**725**[a,b]	**727**[b]	**730**[a,b]	**737**[b]	**752**[b]	**847**[b]
Hap10[c]	T	E	V	I	L	P	F	I	G	V	R	N	Q	L	E	V	R	M
**001*[d]			V	I	L	P	F			V	R	N	Q	L	E	V	R	M
Hap10[e]		E				P		I	G	V	R	N	Q		E			

[a]Amino acid identified by genotyping/imputation
[b]Amino acid identified by sanger sequencing of full-length cDNA of *ERAP1*
[c] Full-length cDNA (Allotype) amino acid sequence obtained from two Birdshot uveitis patients heterozygous and homozygous for *Hap10* in this study.
[d]Allotype name and amino acid positions adapted from [37]
[e]Allotype name and amino acid positions adapted from [34]